Dissolved Organic Carbon Mobilization and Degradation Patterns in Retrogressive Thaw Slumps of the Peel Plateau, Northwest Territories, Canada

by

Cara Aileen Bulger

A thesis submitted in partial fulfillment of the requirements for the degree of

Master of Science

in

Ecology

Department of Biological Sciences
University of Alberta

Abstract

Anthropogenic climate change has affected the Canadian Arctic cryosphere, accelerating the development of retrogressive thaw slumps (RTS) across the Peel Plateau, NWT, Canada. RTS result from the thawing of ice-rich permafrost and develop due to ablation of ground ice exposed in the slump headwall. RTS provide pathways for dissolved organic carbon (DOC), previously inaccessible when stored in permafrost, to become available for biologically or photochemically-mediated degradation; creating a relatively novel input source to the global carbon cycle. The Peel Plateau, which is comprised of ice-rich glaciogenic materials and soils that are rich in inorganic materials, exhibits a high occurrence of RTS activity. RTS activity in the Peel Plateau is predicted to alter the carbon dynamics of receiving waters in ways that contrast with the effects of permafrost slumping in Arctic regions containing organic-rich soils. Here, we explore the environmental drivers and absolute magnitude of DOC delivery to impacted stream systems, and the susceptibility of this DOC to biological degradation. This work determined that temperature and precipitation are the main drivers of DOC mobilization across the Peel Plateau; environmental variables that are predicted to increase considerably across Arctic regions. Pristine streams demonstrated higher concentrations of DOC than streams impacted by slump runoff, an effect that seems likely to occur as a results of DOC adsorption to slump particles. DOC from RTS streams was more susceptible to bacterial degradation, though at lower rates than those found in other thermokarst impacted regions. Spectral and isotopic characteristics of RTS-affected and pristine streamwater were examined to explore how differences in DOC origin and composition relate to decomposition. Permafrost DOC response to climate change has been identified as one of the key knowledge gaps in predicting how integrated Arctic systems will function in the future. This work aimed to close this gap through the monitoring of the flux and fate of DOC mobilized from slump features in an understudied region.

Preface to the Thesis

This thesis is an original work by Cara Aileen Bulger and is divided into four distinct chapters. The first chapter is an introductory chapter that provides background to the region and field of study, outlines research objectives and general experimental methodology. Chapters two and three are written in manuscript format. Citation structure for publication submission is provided below. The final chapter provides concluding statements drawn from this research and proposes avenues of future research. This thesis is written in the plural as science is a team sport and this work was a collaborative effort.

Chapter Two

Bulger, C.A., Tank, S.E. and Kokelj, S.J. The effect of retrogressive thaw slumps on dissolved organic carbon delivery to streams of the Peel Plateau, NWT, Canada

Chapter Three

Bulger, C.A. and Tank, S.E. Unique trends in the biodegradability of dissolved organic carbon mobilized from retrogressive thaw slumps on the Peel Plateau, NWT, Canada

Acknowledgements

The list of people I would like to acknowledge for helping me throughout my Master's degree is lengthy but I would like to begin with my supervisor, Dr. Suzanne Tank. Suzanne has been the most intelligent, reasonable, rational, insightful, motivating, and supportive supervisor throughout the duration of my degree. Her support and encouragement in developing my research project and academic skills have been essential. I would also like to thank Dr. Shelley Hunt for supporting me since the beginning, and encouraging me to explore graduate school. I would like to acknowledge Steve Kokelj, who directed us to the thaw slumps in the first place and offered some much needed guidance before our first field season. I would also like to thank members of my supervisory committee, Rolf Vinebrooke and Vincent St. Louis for helping bring my thesis to completion. Mingsheng Ma (Biogeochemical Analytical Service Laboratory, U of A) and Jackson Langat (Biogeochemical Lab Facilities, York University) were crucial to this degree and are much appreciated for their knowledge and help during lab analyses.

This research was undertaken on Gwich'in traditional lands and I would like to thank Fort McPherson Northern Resources Office and residents for allowing us to discover, explore and observe their beautiful lands. Environment Canada and the NWT Geosciences Office also provided meteorological data integral to my research. Financial supported has been provided by Northern Scientific Training Program, NSERC Discovery and Northern Research Supplement, Polar Continental Shelf Program, Ontario Graduate Scholarship, York University Graduate Teaching Assistantship, and University of Alberta Graduate Teaching Assistantship.

Throughout my degree my family has supported me in many different ways and are always there for me, especially my mum, Carol, who has listened to more statistics-based rants than she ever hoped to in her lifetime. I'd also like to thank Rocky, who tried to learn how to read a map to help out, and my brother, Brendon, who has offered creative solutions and ideas throughout the years, which have been much appreciated.

This degree would not have been the same without the friends I have met along the way. Scott Zolkos, has been the wittiest field comrade and lab mate, and helped chase away that bear. Sarah Shakil has been a great support, valued my advice and 'expertise' and posseses excellent map making skills.

Chelsea Willis has partaken in many escapades and while being such an amazing friend, even if she does steal dog sitting gigs. Lindsay, Allison, and David have been delightful and engaging office mates who have made working at the U of A that much better. Last but certainly not least, I would like to thank my partner, Etienne, who provided motivation when I needed it the most.

Thanks for everything; it's been quite the adventure.

"So these *things*, what are they supposed to help the numbers do?"

- My mother, Carol, on statistics

Table of Contents

List of Figures

List of Tables

1.0 General Introduction

1.1 Climate change in Arctic regions

The Arctic has been experiencing unprecedented changes in its climatic patterns, most notably in observed and predicted increases in temperature and precipitation (IPCC, 2014). Arctic regions are particularly vulnerable to climate change due to the presence of permafrost, ground that remains below 0^{o}C for longer than two years. Permafrost provides mechanical stability to the landscape, maintains landscape-level processes, and controls the hydrological connectivity of terrestrial and aquatic systems. Models assessing impacts of climate change predict an increase in permafrost temperature and thawing, however these predictions contain high levels of uncertainty, with significant disagreement amongst models (Hinzman et al., 2013). When permafrost thaw occurs it can manifest in diverse ways; as a gradual top-down thaw deepening the active layer, or a more rapid degradation of the permafrost in the form of thermokarst (Schuur et al., 2008). Thermokarst is the formation of landscape collapse features as a result of ice rich permafrost thaw (van Everdingen, 2005);different thermokarst features manifest with varying in degrees of severity. Thermokarst features include active layer detachments, which result in the downslope removal of the active layer, thermal erosion gullies and ice wedge polygons formed as a result of channelized surface water, and retrogressive thaw slumps which are mass wasting events on the landscape caused by a complete destabilisation of the ice-rich permafrost below (Kokelj & Jorgenson, 2013). Thermokarst features provide rapid pathways for organic carbon previously inaccessible while stored in permafrost to become available for either processing within soils, where it is then microbially or photochemically degraded, or loss through downslope transport. This carbon mobilization is a key area of research in the Arctic, and the response of dissolved organic carbon (DOC; see below) to changing climate regimes and permafrost degradation has been identified as one of the greatest knowledge gaps and therefore the ability to predict further changes in Arctic regions (Abbott et al., 2016).

1.2 Retrogressive thaw slump morphology

Retrogressive thaw slumps occur when massive ground ice within ice-rich terrains degrades. This process removes surface organic soil layers, exposes mineral soils, and drastically alters the local hydrology, and sediment and solute fluxes (Kokelj et al., 2009). Retrogressive thaw slumps are pulse disturbances that can persist for decades and greatly impact local freshwater systems (Kokelj &

Jorgenson, 2013; Vonk et al., 2015a). Many factors influence slump development, including ground ice content, topography, slope degree and aspect, and regional climate (Lewkowicz, 1990; Kokelj & Jorgenson, 2013; Kokelj et al., 2015). Slumps are polycyclic in nature and can become stabilized when thawed sediment accumulates at the base of the headwall, covering the ground ice and protecting it from further degradation. Slump development can be reactivated through extreme rainfall and other mass wasting events (Burn & Lewkowicz, 1990; Lantuit & Pollard, 2008; Kokelj et al., 2015). There has also been a positive feedback cycle identified within thaw slump features, where the headwall conditions influence the microclimate through increasing local temperatures, further propagating ablation and thaw slump development (Grom & Pollard, 2008). As of 2015, there are 212 thaw slumps identified on the Peel Plateau, 89% of which are currently active (Lacelle et al., 2015).

Thaw slumps are comprised of three main zones: 1) a near vertical head wall; 2) an accumulation zone; and 3) the debris flow (Lewkowicz, 1987). The headwall exposes the active layer and subsisting ice-rich permafrost and can be tens of meters deep in this region (Lewkowicz, 1987). The accumulation zone at the base of the headwall is less steep but can still expose ice rich permafrost or be comprised of previously eroded materials that have not yet been removed. The extent of the accumulation zone impacts stabilization rates. The debris flow is comprised of thawed permafrost and mixed with the fallen active layer, travels downslope and can extend numerous kilometers (Lewkowicz, 1987). Thaw slumps can directly impact substantial land areas; the average thaw slump on the Peel Plateau is 5.4 ha, with the largest one recorded at 52 ha in area (Lacelle et al., 2015).

1.3 Dissolved organic carbon

Previous characterizations of carbon dynamics have neglected the role of freshwater systems, leading to an imbalance in the quantification of the global carbon cycle (Cole et al., 2007; Aufdenkampe et al., 2011). DOC is an important component to quantify as an estimated 80% of total riverine organic carbon flux in the Arctic is predicted to be in the form of DOC (Spencer et al., 2015). A portion of the DOC pool will be realeased from permafrost stores, which is a novel source and expected to be easily degraded, changing local carbon dynamics (Battin et al., 2008; Vonk et al., 2013a). DOC is one of the main controls on microbial metabolism as it can be easily transported through cell membranes, in contrast with organic carbon in the particulate form, which must first be lysed via extra-cellular enzymes (Hanson et al., 2003; Striegl et al., 2005). DOC is considered a crucial transitional phase in the global carbon cycle through its governance on the rate at which permafrost carbon is degraded and released to the

atmosphere (Vonk et al., 2013a, 2015b). The lability of permafrost DOC is expected to be greater than contemporary sources of terrestrial DOC in the Arctic, many potential hypotheses are presented to explain this greater lability; one of the most prevalent is the incomplete microbial degradation prior to permafrost sequestration, compared to terrestrial DOC that has participated in abundant processing within the shallow active layer (Khvorostyanov et al., 2008a; Schuur et al., 2008; Abbott et al., 2014; Vonk et al., 2015b). Rivers and stream networks are ultimately responsible for the transport of DOC and numerous transformations occur during transportation. The role that stream networks play in carbon cycling will only become more important in the future as the hydrological connectivity between Arctic terrestrial and aquatic systems is predicted to increase (McGuire et al., 2009; Schuur et al., 2013). DOC also controls important ecosystems processes within the water column such as light absorption and the transfer and availability of energy, nutrients, and contaminants, therefore any perturbations can have ripple effects on ecosystem functioning (Lee & Kuo, 1999; Weishaar & Aiken, 2003; Spencer et al., 2009).

1.4 Retrogressive thaw slumps and DOC mobilization across the pan-Arctic

Retrogressive thaw slump features are found throughout the world's permafrost influenced regions, including in Canada (Kokelj & Jorgenson, 2013), Siberia (Vonk et al., 2013b), Alaska (Jorgenson et al., 2006), Antarctica (Oliva & Ruiz-Fernández, 2015) and China (Jin et al., 2007). The western Canadian Arctic is particularly susceptible to intense thermokarst resulting in massive retrogressive thaw slumps, as result of widespread glaciogenic deposits and fine grain mineral till in this region (Mackay, 1971). Soil in this region is carbon poor (Hugelius et al., 2014), and covered with thick till deposits (Hughes et al., 1972; Duk-Rodkin & Hughes, 1992) and is unique from a research perspective as the vast majority of research on DOC flux and degradation from degrading permafrost has been conducted in organic-rich regions with high carbon content (Frey & Smith, 2005; Neff et al., 2006; Mann et al., 2012; Vonk et al., 2013b; Drake et al., 2015). These soil differences have led to two potential hypotheses for global DOC response to permafrost thaw: 1) thawing permafrost will lead to increased water flux through mineral soils and decreased DOC export to aquatic systems, or conversely, 2) permafrost thaw will expose high levels of carbon for export (Frey & McClelland, 2009; Tank et al., 2012; Hinzman et al., 2013). These two hypotheses are not mutually exclusive; the underlying geology and presence and depth of peat and organic soils influence whether or not the region experiencing permafrost degradation will be a source

of carbon export. These regional differences, and their influence on DOC mobilization, require the Arctic to be investigated as the heterogeneous landscape that it is.

1.5 Study rationale and hypotheses

This research seeks to examine the impact of thaw slumps on DOC delivery to stream ecosystems at eight slump sites across the Peel Plateau (Fig. 1.1), and to assess the fate of DOC released by thaw slumps using experimental manipulations. This research attempts to gain a full understanding of the pathways and fates of DOC released from retrogressive thaw slumps by thoroughly examining the degradation of slump-released DOC in controlled laboratory incubations, and by measuring differences in DOC concentration and flux upstream and downstream of slump sites (Fig. 1.2). This research also endeavours to determine a possible correlation between environmental conditions and the rate at which DOC is released from slumps. The following hypotheses were developed to address these objectives:

1) If deepened flowpaths or increases in suspended inorganic materials occur as a result of slump activity then within-slump outflow and downstream locations will see decreased DOC concentrations compared to upstream DOC values (see Kokelj et al. (2005) for similar work in upland lakes). It was hypothesized that the mineral soils of the region would impact DOC dynamics, contrary to trends seen in regions with organic rich soils.
2) Environmental parameters correlated with slump initiation and development (Lewkowicz, 1986, 1987; Kokelj et al., 2009, 2013, 2015; Lacelle et al., 2010) will also be important predictors of DOC flux from thaw slumps.
3) If the presence of slumping significantly affects the origin of streamwater DOC then rates of within-slump and downstream DOC biolability will increase relative to upstream locations. It is hypothesized that this will occur because the release of previously sequestered carbon will change the pool of DOC available for in-stream degradation. An increase in DOC lability is predicted as the DOC locked in permafrost has been found to be more labile than active-layer derived DOC in other regions (Woods et al., 2011; Cory et al., 2013; Vonk et al., 2013a, 2015b; Fritz et al., 2015; Mann et al., 2015).

1.6 Study design

Survey sampling was undertaken at eight thaw slumps across the Peel Plateau, NWT (Figs. 1.1 and 1.3).

To map the effect of slumps on streamwater concentrations of terrestrially-derived DOC a comparison of upstream, downstream and within slump outflow DOC concentrations was conducted (Fig. 1.2). An extensive sampling regime was carried out at one slump (Fig 1.3; FM3) and correlated with meteorological data from a nearby weather station (Fig. 1.1). To determine the amount of DOC that is biologically degradable in slump-affected versus unaffected ecosystems, bacterial manipulations were constructed to determine the biolability of the carbon (Vonk et al., 2013a). Degradation incubations were constructed to best mimic environmental conditions present at the time the carbon is introduced into the aquatic ecosystem from degraded permafrost, and conditions that can be expected in downstream environments. These measures of biodegradability establish the impact slump-derived DOC has on the biogeochemistry of stream ecosystems and, ultimately, its potential fate in downstream systems such as the Arctic Ocean (Holmes et al., 2008).

1.7 Significance

As a result of the increase in abundance and magnitude of permafrost disturbances, thermokarst features are being recognized as an important biophysical variable influencing greenhouse gas exchange in the North (Abbott et al., 2016), especially at small headwater streams, which have been identified as important sites for microbial activity, through CO_2 outgassing (Spencer et al., 2015). This research seeks to map the linkage between terrestrial to aquatic carbon pools, and describe how this will impact aquatic ecosystem functioning and local carbon dynamics in a region where the presence of mineral-rich soils could significantly affect land to water carbon transfer. DOC fluxes explicitly show how slump presence impacts carbon mobilization within stream ecosystems, while biodegradable DOC (BDOC) incubations demonstrate the potential degradability of DOC. A thorough understanding of the impacts of permafrost thaw on northern aquatic ecosystem functioning is fundamental to creating correct projections for future climates, and for understanding the feedback cycles between permafrost thaw and climate to mitigate the effects of climate change (Battin et al., 2008; Spencer et al., 2015).

1.8 Figures

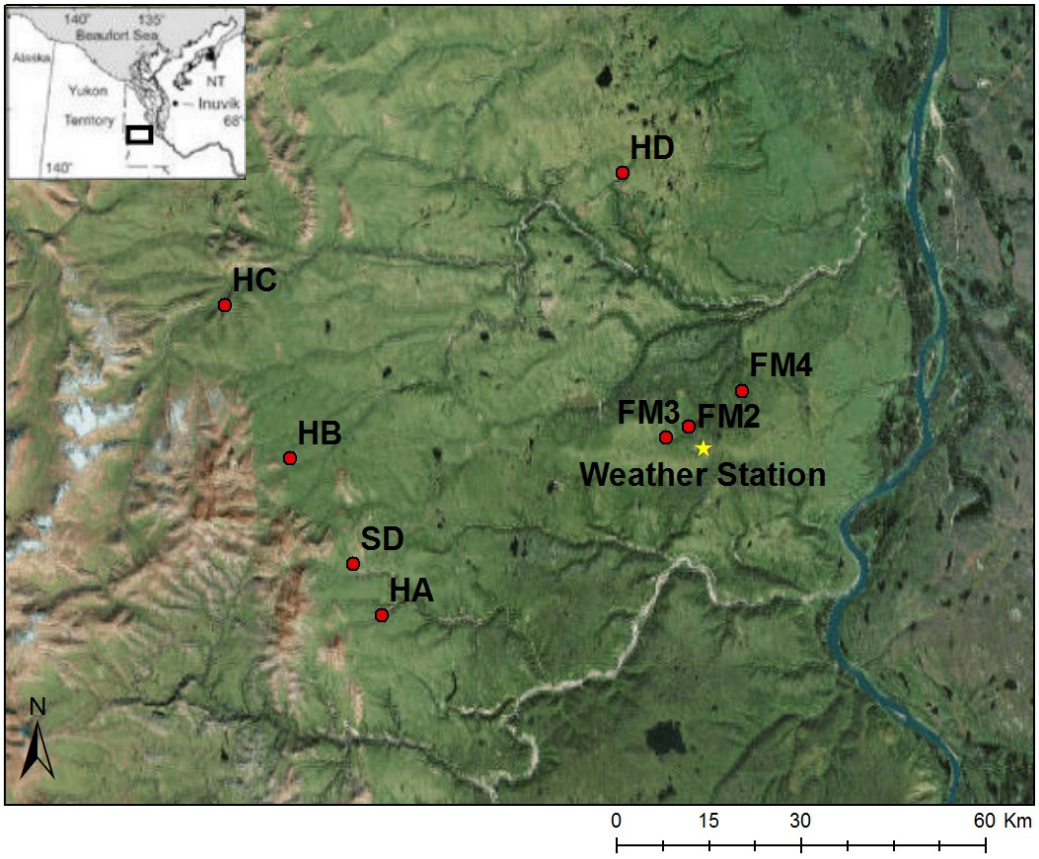

Figure 1.1 Locations of the eight studied retrogressive thaw slumps on the Peel Plateau, Northwest Territories, Canada, sampled throughout July and August 2014 (Inset adapted from Kokelj & Burn (2003)). Sites HA, HB, HC, and HD are helicopter access sites and FM2, FM3, FM4, and SD are walk in accessible sites from the Dempster Highway. Slump FM3 was selected for the environmental correlation objective.

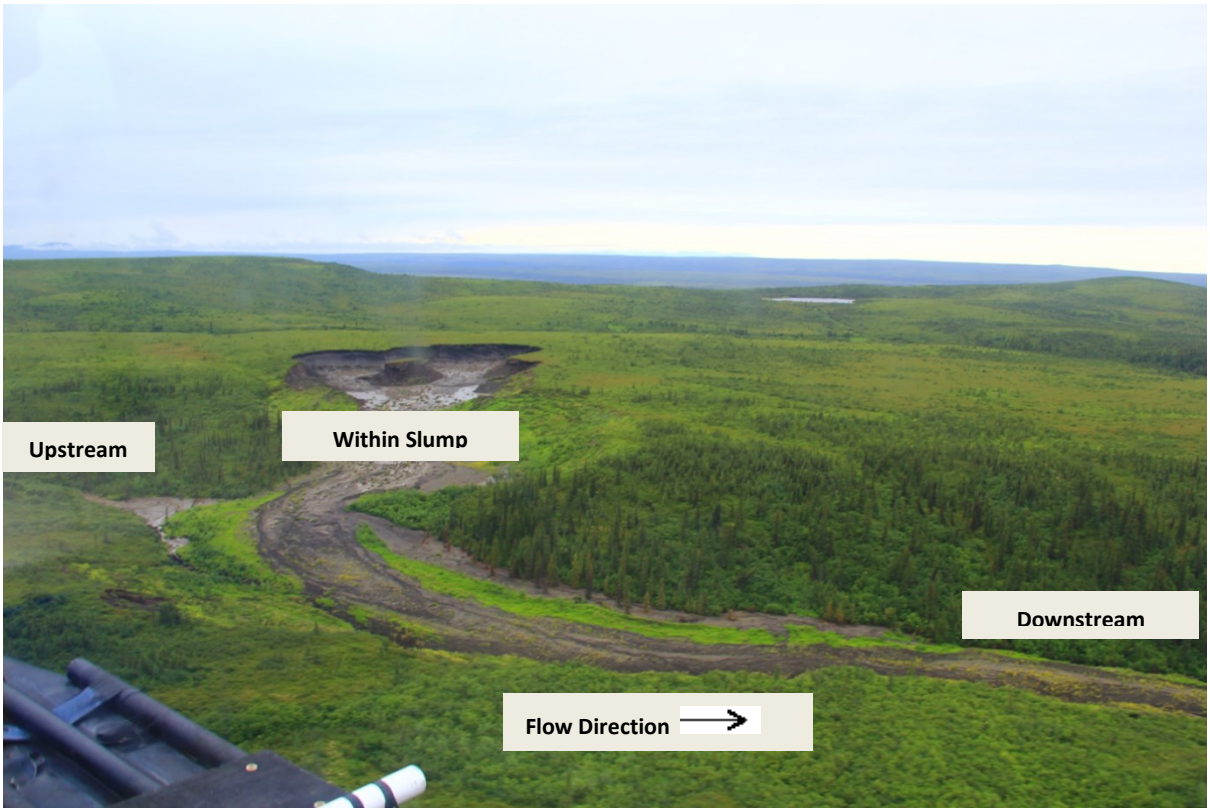

Figure 1.2 Sampling locations at retrogressive slump sites; FM3 depicted. Upstream sites are pristine environments, uninfluenced by any disturbance. Within slump sampling locations are channelized flowpaths within the slump runoff. Downstream sampling locations are located beyond the point of upstream and within slump flowpath convergence and were selected to be representative of slump impacts on aquatic ecosystems.

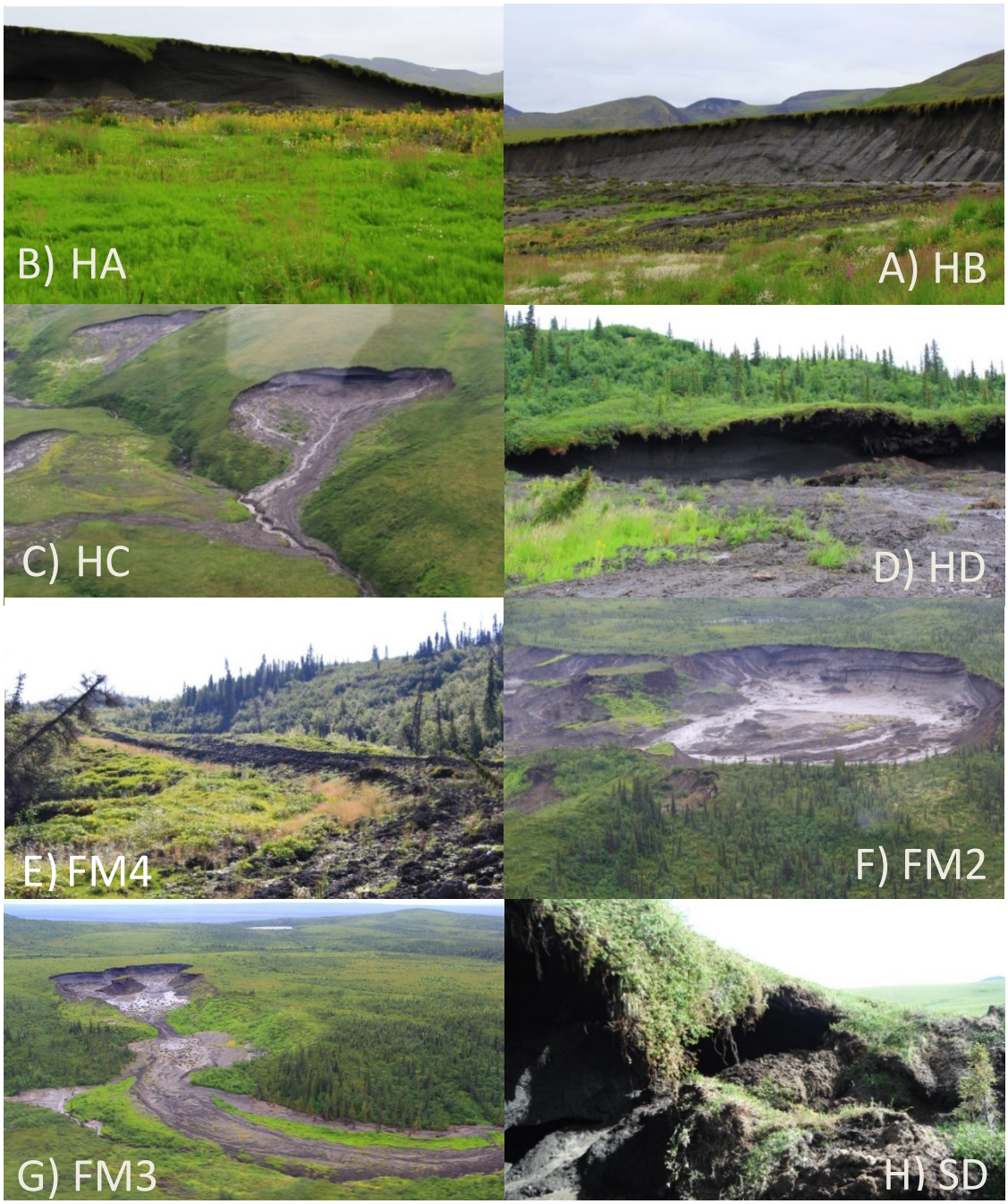

Figure 1.3 Images of the eight individual retrogressive thaw slumps sampled over the 2014 summer field season. A) Slump HA with revegetated scar zone B) Slump HB showing ice-rich headwall C) Slump HC (furthest on the right) with a large active scar zone and debris tongue D) Slump HD, smaller, with an overhanging active layer adjacent to a larger stream E) Slump FM4, shows revegetating debris tongue of a recently stabilized mega slump F) Slump FM2, an active mega slump, with numerous lobes (largest lobe shown) G) Slump FM3, an active mega slump, location of environmental correlation sampling H) Slump SD, recently initiated by stream erosion. Photograph shows a shallow headwall and a large overhanging active layer.

2.0 The effect of retrogressive thaw slumps on dissolved organic carbon delivery to streams of the Peel Plateau, NWT, Canada

2.1 Introduction

Anthropogenic climate change has been affecting the Arctic cryosphere, and with northern temperature increases predicted to be at least 40% greater than the global mean these changes will only be exacerbated in the future (IPCC, 2014). Most notably, temperature and precipitation are expected to increase significantly in the Arctic (Walsh et al., 2011; IPCC, 2014). One way in which changing climate affects northern regions is through its impacts on permafrost stability, as permafrost is vulnerable to climatic perturbations and is an integral part of the landscape (Khvorostyanov et al., 2008a, 2008b; Schuur et al., 2008, 2013; Frey & McClelland, 2009). Permafrost acts as a long term storage unit for solutes, including dissolved organic carbon, and as a barrier to active participation within biogeochemical cycles (McGuire et al., 2009). One of the major changes predicted and observed in northern regions is the increased linkage between terrestrial and aquatic systems, via the alteration of hydrological pathways and increasing transport of terrestrial compounds (Frey & McClelland, 2009; Vonk et al., 2015a). Links between terrestrial and aquatic carbon pools have previously been ignored when calculating global carbon budgets. However, in recent years, the importance of this link for greenhouse gas exchange, sediment accumulation and carbon transport has been noted (Cole et al., 2007). With global permafrost stores of carbon estimated at 1670 Pg, double that of the atmospheric carbon pool, there is great potential for large increases in carbon transport and degradation through permafrost perturbation (Hugelius et al., 2014).

Dissolved organic carbon (DOC) is the primary substrate controlling microbial metabolism, the main control for carbon dioxide release to the atmosphere (Battin et al., 2008; Spencer et al., 2015). Measuring DOC input to river ecosystems is important as northern rivers deliver large amounts of terrestrial DOC to Arctic Ocean coastal and ocean environments (Dittmar & Kattner, 2003; Wickland et al., 2012), making quantification of this carbon an important input variable for the construction of accurate landscape and oceanic carbon budgets.

Permafrost degradation leads to an increase in the conduct and processing of solutes and carbon along the land-to-freshwater continuum, and can manifest in many different forms across the landscape

(Kokelj & Jorgenson, 2013; Malone et al., 2013; Abbott et al., 2014, 2015). Permafrost features are influenced by factors such as topography and local ground ice content (Kokelj & Jorgenson, 2013). One of the most conspicuous manifestations of permafrost thaw is the retrogressive thaw slump, which occur in regions with large expanses of ice-rich terrain. Thaw slumps in the western Canadian Arctic can grow to enormous proportions and are incredibly dynamic, with headwalls extending deep into permafrost horizons, and outflows that drastically alter the geochemistry of downstream, impacted fluvial systems (Kokelj et al., 2013; Malone et al., 2013; Abbott et al., 2014, 2015).

Retrogressive thaw slumps are widespread across the Peel Plateau (Lacelle et al., 2015) and geochemical impacts from thaw slump activity can be seen at large scales (i.e., 70, 000 km^2 watershed; Kokelj et al., 2013). Impacts on receiving water geochemistry are observed even when a small portion (<30%) of a region is influenced by large thermokarst disturbances (Kokelj et al., 2005). Other studies have found that increases in solute load in regions affected by permafrost disturbance can be transient (i.e., during spring freshet) and have little influence on the annual solute loads (for example, in High Arctic regions affected by active layer detachments; Lafrenière & Lamoureux, 2013). In contrast, retrogressive thaw slumps have a much greater impact on stream geochemistry owing to their vast size and depth, with impacts that have been seen in large watersheds and major rivers fed by thermokarst disturbed regions (Kokelj et al., 2013).

Permafrost thaw enables DOC transport to streams (Walvoord & Striegl, 2007; Frey & McClelland, 2009; Vonk & Gustafsson, 2013), however regional soil composition can influence how DOC is mobilized from land to stream ecosystems. The potential for adsorption to soil particles is much greater in regions that contain mineral soils when compared to regions with organic rich soils, which are less likely to sequester carbon (Frey & Smith, 2005; Kothawala et al., 2008; Vonk et al., 2013a). The western Canadian Arctic is comprised of carbon-poor glaciogenic mineral soils (Mackay, 1971; Duk-Rodkin & Hughes, 1992) that have high intrinsic adsorption properties and therefore a high potential for carbon sequestration (Kothawala et al., 2008). The majority of permafrost DOC research has been conducted in regions with organic-rich soils (Vonk et al., 2013a, 2013b; Drake et al., 2015), therefore DOC released from permafrost on the Peel Plateau is predicted to contrast these previously observed trends.

This is one of the first studies endeavouring to quantify the impact that changing environmental conditions will have on DOC mobilization from thermokarst features in the western Canadian Arctic. Kokelj & Jorgenson (2013) have noted the knowledge gap in the understanding of environmental drivers of slump development and this uncertainty extends to influences on DOC flux. Variation in temperature,

precipitation, and solar radiation has been correlated with rates of development and growth of retrogressive thaw slumps and is predicted to also control the release of organic carbon from thaw slumps (Lewkowicz, 1986, 1987; Kokelj et al., 2009, 2013, 2015; Lacelle et al., 2010).

This paper seeks to clarify DOC transfer from terrestrial to aquatic systems impacted by retrogressive thaw slumps on the Peel Plateau (Striegl et al., 2005; Frey & McClelland, 2009). The objectives of this study are to 1) determine the effects of retrogressive thaw slumps on the concentration and composition of DOC in slump-affected streams of mineral rich regions and 2) determine the sensitivity of thaw slump carbon release to fluctuations in the environmental conditions of precipitation, temperature and solar radiation. It is expected that deepened flowpaths and increases in suspended inorganic materials will occur as a result of slump activity, and therefore lower DOC concentrations will be present in slump impacted waters due to the increased contact between DOC and mineral soils. Precipitation and temperature increases have been correlated with slump initiation and development and are predicted to be the primary drivers in DOC flux from both the landscape and thaw slumps.

2.2 Study site

2.2.1 General study site description

All studied thaw slumps were located on the Peel Plateau, situated in a continuous permafrost zone in the eastern foothills of the Richardson Mountains, NWT, Canada. The Peel Plateau is gently sloping and predominately eastern facing with elevations ranging from 100 to 650 m.a.s.l. (Catto, 1996). The region was covered by the Laurentian Ice Sheet (LIS) 18,500 cal yr B.P. for a brief period (Lacelle et al., 2013). The bedrock of the region is Lower Cretaceous marine shale from the Arctic River Formation (Norris, 1984) and siltstone overlain by Late Pleistocene glacial, glacio-fluvial and glacio-lacustrine sediments (Duk-Rodkin & Hughes, 1992), covered by a shallow organic layer. Carbon dating and ^{18}O values in the region have placed the age of regional ground ice in the late Pleistocene epoch (18,100 ± 60 ^{14}Cyr BP; Lacelle et al., 2013). Upper layers of the permafrost profile, delineated by a thaw unconformity, have been aged as early Holocene (7890 ± 250 ^{14}Cyr BP; Lacelle et al., 2013). The thaw unconformity developed as a result of a warmer climate in the early Holocene that prompted a deepening of regional active layers; increased saturation of the ground resulted in identifiable variations in the ground ice cryostructure and greater incorporation of organic matter into soils (Murton & French, 1994; Kokelj et al., 2002). The mineral rich soil present in the western Canadian Arctic sharply contrasts that of Yedoma soils found throughout much of Beringia, where a third of organic carbon stored in permafrost regions is

estimated to reside and significant slump activity has also been observed (Vonk et al., 2013b; Hugelius et al., 2014).

The development of thermokarst features across the Peel Plateau is influenced by the thermal instability of the active layer, which is primarily driven by annual thaw and ground ice content (Lantuit & Pollard, 2005); this fine grain mineral till of this region also facilitates thaw slump development. Ongoing fluvial processes and stream network expansion also increase thaw slump activity (Lacelle et al., 2015). The extent of the LIS directs the distribution of RTS across the Peel Plateau, with no slumps present beyond its glacial limits. The presence of the LIS terminus has been correlated with large layers of buried ice within the top layer of permafrost (Lacelle et al., 2015). Two hundred and twelve thaw slumps were recently identified across the Peel Plateau region, 89% of which are currently active (Lacelle et al., 2015). Slump size ranges from small, newly developing features, which are relatively numerous, to those greater than 20 ha, which are rare (<5% prevalence; Lacelle et al., 2015).

2.2.2 Regional climate

The regional climate is typical of subarctic regions with long, cold winters and short, cool summers. Mean annual air temperature (1981-2010) at the Fort McPherson (Fig. 1.1) weather station is -7.3°C with average summer (June-August) temperatures of 13.3 °C (Environment Canada, 2015). A warming trend of 0.77 °C per decade since 1970 has been recorded; however these increases are most apparent in the winter months (Burn & Kokelj, 2009). Our sample period spanned the thaw months of July and August; average 1981-2010 temperatures for those months, recorded at Fort McPherson, are 15.2 and 11.8 °C, respectively, slightly higher than averages observed during our study (13.2 °C in July and 9.5 °C in August). Annual cumulative precipitation (1981-2010) averages 145.9 mm, with July and August having the highest rainfall levels at 46.4 and 39.1 mm, respectively (Environment Canada, 2015). In 2014, rainfall for July and August was 128.7 and 170.7 mm. This makes 2014 a cooler year than average, and continues the trend of increasingly wetter summers with numerous extreme rainfall events (Kokelj et al., 2015).

2.3 Methods

2.3.1 Slump site selection

Eight thaw slumps were selected from across the study region (Fig. 1.1; Table 2.1). Three slumps were accessed from the Dempster Highway three times over the sampling season, four were accessed twice

via helicopter and one slump (FM3) was accessed in concert with the road-access sites, and an additional 16 times to assess the effects of environmental variation on carbon flux from slumps. Slumps selected for sampling possessed a debris tongue that extended to the valley bottom and directly impacted a stream system. Sampling at each slump occurred at three discrete locations: upstream, within-slump, and downstream of the slump influence (Fig. 1.2). Upstream sites chosen were streams connecting with the slump flow path further downstream, and were un-impacted by any disturbances. Thus, this sampling location was representative of an undisturbed, pristine environment. Within-slump sampling locations chosen possessed a clear channelized flow of slump runoff, located within the main body of the disturbance at the beginning of the debris tongue. Downstream sampling locations were located below the confluence of the upstream flow and all within-slump runoff paths and are representative of slump impact on aquatic ecosystems across the Peel Plateau landscape. In one instance, (Slump HD, August 17) a massive change in slump morphology between sampling periods caused a loss of within-slump channelized water flow. As a result, the within-slump sample taken at this site was not representative of typical slump outflow, and has been discarded from our analyses.

A general classification of the slumps is difficult as they are incredibly diverse (Table 2.1; Fig. 1.3). Three of the slumps (FM4, FM2, FM3) are classified as 'mega slumps', characterised by areas greater than 5 ha and a headwall greater than 4 m in height (Kokelj et al., 2013, 2015). FM4 is the largest of the thaw slumps in area, with a headwall approximately 20 m in height; however most of the slump is stabilized, indicated by the small outflow, long, dry debris tongue and significant vegetation present on the tongue. FM2 geochemistry and geomorphology were well outlined in Malone et al. (2013). This slump is considered to be one of the largest active slumps in the region, with a headwall approximately 25-30 m high and slump area that has been visible in air photos since 1944 (Kokelj & Jorgenson, 2013; Malone et al., 2013). Slump FM3, which was chosen for our 'environmental controls' work (see below) has been well characterized by Kokelj et al. (2015). This slump covers an area of approximately 10 ha and has a headwall of approximately 10 m (Kokelj et al., 2015; Lacelle et al., 2015). Headwall retreat rate at FM3 over a 20 year period was calculated to be 12.5 m yr^{-1} (Lacelle et al., 2015); slightly higher than the average retreat rate reported for the Peel Plateau (12.1 m yr^{-1}; Kokelj et al., 2013). SD is the smallest slump in the study and the most recently initiated, following the diversion of a small creek. The SD headwall is 2-4 m tall and the slump outflow extends approximately 20 m, with no defined debris tongue. The helicopter access sites (HA, HB, HC, and HD) were all well established, active thaw slumps with headwalls of approximately 10-15 m and well-defined debris tongues (Fig. 1.3). With the exception

of SD, slump headwalls extend below the thaw unconformity, thus exposing Pleistocene-aged sediments and ground ice (Lacelle et al., 2013).

2.3.2 Sampling and data collection

At each sampling location, conductivity, pH, and temperature were recorded using a YSI Pro Plus multi-parameter meter outfitted with a Quattro cable. Water samples were collected from directly below the stream surface into 1 L acid washed high-density polyethylene (HDPE) bottles and allowed to sit in chilled, dark conditions for 24 hours to enable the substantial sediments to settle out of suspension. Sample water was then filtered with pre-combusted (475°C, 4 hours) Whatman GF/F filters (0.7 µm pore size). Filtered sample water was then transferred into 40 mL acid washed, pre-combusted glass bottles for DOC analysis, or 60 mL acid washed HDPE bottles for the analysis of absorbance and major ions. DOC samples were acidified with hydrochloric acid (1 µL mL^{-1}), following Vonk et al. (2015b). All samples were kept refrigerated until analysis. The GF/F filters were retained for total suspended sediment (TSS) analysis. Samples for stable water isotope analysis were collected directly from streams into acid washed 40 mL HDPE bottles with no headspace. Bottles were sealed and refrigerated until analysis.

To calculate DOC flux (concentration/discharge) at slump FM3, discharge was measured at the upstream and downstream sites for this slump. The cross sectional method was used to measure both upstream and downstream discharge. Downstream flow was measured using an OTT C2 current meter, at three locations across the small stream and 40% depth. Due to the low flow conditions at the upstream site, upstream flow was measured by dividing the stream into tenths and floating a buoyant object and determining the time it took to float a specified distance (Ward & Robinson, 2000).

Local, fine-scale climate data were obtained from an automated meteorological station previously established in 2010 by the Government of the Northwest Territories (Kokelj et al. 2015). The station is located within 2 km of the FM3 site (Fig. 1.1) and is instrumented for the measurement of air temperature, rainfall, and net radiation. These data were used for the environmental control work described below.

2.3.3 Laboratory analyses

2.3.3.1 Major ions, dissolved organic carbon and $\delta^{18}O$

Cation concentrations (Ca^{2+}, Mg^{2+}, Na^{+}) were analyzed on a Perkin Elmer Analyst 200 Atomic Absorption Spectrometer at York University. Cl^{-} concentration was determined using a Technicon Continuous Flow Analyzer. These parameters were measured as they have high utility as indicators of permafrost

disturbance in this region (Kokelj et al., 2005, 2013; Thompson et al., 2008; Malone et al., 2013). A subset of collected samples were analyzed for total dissolved Fe at the University of Alberta on an Inductively Coupled Plasma - Optical Emission Spectrometer (Thermo Scientific ICAP6300), to allow for the correction of our Specific UV Absorbance results (see below). DOC samples were analyzed on a Shimadzu TOC-V analyzer; DOC was calculated as the mean of the best 3 of 5 injections with a coefficient of variance of <2%. A Picarro liquid water isotope analyzer was used to measure stable water isotope samples at the University of Alberta. The precision of each analysis is ± 0.2% for $\delta^{18}O$.

2.3.3.2 Total suspended sediments

Samples for TSS were filtered in the field for later analysis, ensuring that there was enough sediment on the pre-combusted (475°C, 4 hours) and pre-weighed GF/F filters. Filters were stored frozen, and dried at 60°C for 8 hours, placed in a desiccator overnight and promptly weighed. TSS was calculated as the difference in filter weight before and after sediment loading, divided by volume filtered.

2.3.3.3 Absorbance spectra

Refrigerated samples were warmed to room temperature immediately prior to scanning. A 5 cm quartz cuvette was used to obtain UV-visible spectra data from 250-750 nm, using a Genesys 10 UV-Vis spectrophotometer. A subset of samples were re-scanned after being allowed to settle as initial scans showed high particle interference during the original scanning. Samples with high absorbance values (absorbance > 3.0 at 250-255 nm or > 0.03 at 700-750 nm), were rescanned using a 1 cm cell to ensure accuracy of scanned values. Differences between rescan and original scan (RS/OS) were 1.0065 SE ± 0.02 (<5% difference). One scan was eliminated due to erroneously high absorbance values.

A baseline correction was undertaken to eliminate potential interference from particles by subtracting the average absorbance between 700 and 750 nm from all wavelengths within a given scan (Green & Blough, 1994). Specific UV absorbance at 254 nm ($SUVA_{254}$) was calculated by dividing the decadal absorbance at 254 nm (m^{-1}) by the DOC concentration (mg L^{-1}). $SUVA_{254}$ values were corrected for Fe interference following Poulin et al. (2014) using maximum Fe concentrations from either upstream, downstream, or within slump sites, using data from laboratory analyses or as reported in Malone et al. (2013). We chose to use maximum (rather than mean) Fe concentrations to ensure that our between-site $SUVA_{254}$ comparisons were conservative, because both $SUVA_{254}$ and Fe are highest in pristine, upstream sampling locations. Absorbance values were converted to Naperian absorption coefficients (a_λ, m^{-1}) by multiplying by 2.303 and dividing by the cuvette pathlength. Spectral slopes between 275 and 295 nm, and 350 and 400 nm ($S_{275-295}$, $S_{350-400}$) were calculated following Helms et al. (2008). Slopes

are reported as positive values to adhere to mathematical conventions. Slope ratios (S_R) were calculated by dividing the calculated slope values of $S_{275-295}$ by $S_{350-400}$. Spectral properties are easily measured and extremely useful as they are good metrics for DOC composition; $SUVA_{254}$ is strongly correlated with dissolved organic matter aromaticity and S_R correlates well with molecular weight (Weishaar & Aiken, 2003; Helms et al., 2008).

2.3.4 Statistical analyses

Statistical analyses were completed in R version 3.1.3 (R Core Team, 2015). R packages used in these analyses were: 'nlme' (Pinheiro et al., 2015), 'lmtest' (Zeileis & Hothorn, 2002), 'lmSupport' (Curtin, 2015), 'car' (Fox & Weisberg, 2011), and 'zoo' (Zeileis & Grothendieck, 2005).

Differences in measured variables (DOC, $SUVA_{254}$, conductivity, temperature, major ions, and pH) between upstream and downstream, or upstream and within sampling locations were evaluated using either paired t-test or a Wilcoxon Signed Rank Test if the data were not normally distributed. The Dunn-Šidák method was applied to adjust alpha levels to ensure Type 1 errors did not occur as a result of multiple comparisons, ($\alpha = 0.0253$); this is a statistically conservative approach. We used this paired t-test/ Wilcoxon approach to ensure that the significant between-slump variability observed did not mask our ability to detect significant effects of slumping at each site.

Using the high-frequency data from FM3, we conducted multiple linear regressions to assess how environmental conditions (rainfall, temperature, solar radiation) and TSS affect upstream and downstream DOC flux. AIC values were used to determine the best variable model to explain patterns in upstream and downstream DOC concentrations (Burnham & Anderson, 2002). Precipitation and soil surface temperature have been shown to be a positive influence on DOC flux across undisturbed permafrost and boreal regions (Prokushkin et al., 2005; Pumpanen et al., 2014); in continuous permafrost regions the impermeable permafrost barrier forces that precipitation to travel through the shallow active layer, which has low sorption capabilities but high hydraulic conductivity that leads to fast transport of carbon across the landscape into fluvial systems, strongly influencing DOC flux (Striegl et al., 2005). As the objective of this model was to parse out variables that influence downstream DOC flux, upstream DOC flux was separated out into a distinct regression analysis as it was a strong predictor of downstream DOC flux that dwarfed all environmental variables. Models of environmental drivers of DOC flux were tested for serial correlation using the auto-correlation function (ACF). Features tested in the model were air temperature, rainfall, net radiation, and sediment concentrations at upstream and downstream sites. Models with variance inflation factors greater than 10 or significant Durbin Watson

test results (indicative of correlated variables; Durbin & Watson, 1950; Hair et al., 1995) were discarded. Residuals were examined to ensure the model was a good fit for the data (Zuur et al., 2009). Cumulative values for environmental variables (i.e., accumulated rainfall in the previous 48, 72 and 120 hours) were tested in the models. However, these values showed a strong positive correlation to one another, and therefore temporally shifted data (i.e., rainfall 48, 72 and 120 hours prior to the DOC flux measurement) were used in the final model.

2.4 Results

2.4.1 DOC concentration across slump sites

Paired upstream-within-slump comparisons showed no consistent difference in DOC concentration, when evaluated across all slump sites ($p=0.1084$; Fig. 2.1, Table 2.2). At some sites (FM4, FM2, and FM3; the mega-slumps) DOC concentrations tended to be lower in samples taken directly from slump runoff, when compared to paired upstream sites (Fig. 2.1). At other sites (HB, HC, and HD), within-slump DOC concentrations were higher than values upstream (Fig. 2.1). This is most likely due to the ground material accessed by the headwalls, with shallower slumps eroding a much larger proportion of the active and organic-rich Holocene layer high in organics, while mega slumps with deep headwalls erode greater proportions of the mineral-rich tills. In contrast to the upstream-within paired comparisons, DOC concentrations declined significantly between upstream and downstream sites, when assessed across all slumps ($p<0.001$; Fig. 2.1; Table 2.2). Across sites, there was significant variation in DOC concentration, and little consistency in the concentration of DOC draining directly from permafrost slumps. Within sites, DOC concentrations were fairly consistent across our 2-3 sampling periods (Fig. 2.1).

2.4.2 Bulk chemistry of pristine waters and slump runoff

To quantitatively assess the effects of slumping on streamwater chemistry, and explore how the input of slump waters affects downstream DOC, we examined concentrations of conservative ions, conductivity and TSS as 'tracers' of slump activity. Major ion (Ca^{2+}, Mg^{2+}, Na^{+}, Cl^{-}) concentrations in slump runoff were considerably greater than in pristine streams (a 2.7 to 11.7-fold increase; Fig. 2.2 c-e; Table 2.2). These patterns were similar, though muted, at our slump-impacted downstream sites, where major ion concentrations were 1.5 to 3.5-fold greater than in pristine streams (Fig. 2.2 c-e; Table 2.2). Average conductivity also increased significantly as a result of slumping ($p< 0.001$; Table 2.2); within-slump sites showed conductivity values that were 9.2-fold greater than upstream sites and downstream sites had conductivity measures 2.6 times greater than upstream sites (Fig. 2.2b). TSS was also statistically

different between pristine and impacted sites ($p < 0.001$; Table 2.2) with TSS levels being 446 fold greater within slumps compared to upstream and 35.7 fold greater downstream compared to upstream (Fig. 2.2a). pH and temperature were measured to further evaluate stream conditions. pH was statistically different between pristine and impacted downstream sites, while temperature had significant differences between upstream-within slump, and upstream-downstream sites ($p<0.01$; Table 2.2). Upstream sites had the lowest pH and temperature values (6.7 ± 0.1 and 5.5^{o}C ± 0.4), within slump sites had an average pH of 6.8 ± 0.1 and 10.2^{o}C ±1.1 temperature, and downstream sites had a neutral pH (7.0 ± 0.1) with intermediate temperatures (6.5 ^{o}C ± 0.5; Fig. 2.2f-g).

To examine whether the considerable input of slump-derived materials had a deterministic effect on in-stream DOC, we further examined the relationship between a subset of our conservative tracers of slump activity (Ca+Mg, TSS and conductivity) and DOC concentration (Fig. 2.3). In each case, there was no discernable relationship between metrics of slump activity and in-stream DOC.

2.4.3 Spectral and isotopic characteristics

Results of our paired comparisons showed significant differences in $SUVA_{254}$ values between upstream and within-slump, and upstream and downstream, sites ($p<0.01$; Table 2.2). Average within-slump $SUVA_{254}$ values were less than half of those observed for pristine waters (Fig. 2.4a). Downstream values were 0.82-fold of upstream $SUVA_{254}$ values.

When comparing within slump and upstream sites, paired comparisons showed $S_{275-295}$ (average difference 0.0055 ± 0.00066), $S_{350-400}$ (avg diff 0.0025 ± 0.00071) and S_R (avg diff 0.17 ± 0.018) to all be greater within-slump. Between downstream and upstream sites, paired comparisons were significant for all slope metrics; with greater downstream values for $S_{275-295}$ (avg diff 0.00082 ± 0.00034) and S_R (avg diff 0.12 ± 0.021); but greater values for $S_{350-400}$ upstream (avg diff -0.0015 ± 0.00053). However the trends for these comparisons were muted compared to the upstream-within-slump comparisons (Table 2.2). Downstream samples, unsurprisingly, lie in between upstream and within slump values, though closer to upstream patterns (Fig. 2.4a-d), with the exception of $S_{350-400,}$ which have downstream values typically less than both upstream and within-slump values (Fig.2.4c). Differences between upstream and downstream absorbance slopes were marginal; consequently, while these differences are present statistically, the ecological impact of these observed differences is debatable as absolute variation in the values was minimal (Fig. 2.4b-c).

The upstream $\delta^{18}O$ stream water signature averaged -20.1‰ ± 0.12, which corresponds to a relatively modern water $\delta^{18}O$ signature for this region (Lacelle et al., 2013). Within-slump $\delta^{18}O$ exhibited an older source signature with average values of -22.7‰ ± 0.72. Within-slump $\delta^{18}O$ values fall between previously-identified endmembers for Pleistocene-aged ground ice for this region (18,100 ± 60 ^{14}Cyr BP) and the modern active layer (Lacelle et al., 2013) and overlap the $\delta^{18}O$ signature of the Holocene diamicton. Within slump features demonstrated greater variation between sites compared to the upstream and downstream $\delta^{18}O$ values, which were both closely clustered around the modern active layer isotopic signature. Slumps FM2, FM3, and HB had the lowest within slump oxygen isotope signatures; values were more depleted than reported values for the Holocene-aged icy diamicton and closer to previously-reported Pleistocene ground ice values. Downstream $\delta^{18}O$ values were typically similar to upstream values with a small influence from the slump feature (-20.7‰ ± 0.21).

To further investigate the influence of water source for upstream, downstream, and within-slump samples across our study sites, we examined the relationship between $SUVA_{254}$ and $\delta^{18}O$. More depleted samples found within slump features had lower $SUVA_{254}$ values than more modern sourced samples (Fig. 2.5). The $\delta^{18}O$ value is expected to be influenced by the depth of the headwall, which controls the origin of material available for transport from the slump feature. Of the mega slumps that were identified in the DOC section (see above) two of these slumps had $\delta^{18}O$ values that were more depleted than the Holocene-aged icy diamicton values reported in Lacelle et al. (2013), demonstrating they were accessing older, Pleistocene aged permafrost.

2.4.4 Patterns and environmental drivers of DOC flux

An examination of the environmental controls on DOC delivery to streams occurred at slump FM3, where, downstream DOC flux (mg s^{-1}) was typically slightly greater than upstream DOC flux. However, when flux values were low, downstream and upstream fluxes were comparable (Fig. 2.6). As a result, paired comparisons indicate no statistical difference between upstream and downstream DOC flux (Table 2.2). Upstream and downstream DOC flux were strongly correlated to one another ($R^2 = 0.94$; $p<0.0001$); therefore the two flux values were separated into two multiple linear regressions to explore environmental controls on each. Time-of-sampling (0h) and temporally shifted (48, 72 and 120 hours prior to sampling) data were used to determine which environmental factors drive DOC mobilization from both the landscape and thermokarst features. As described in the *Methods,* all models met conditions for normality and lack of correlation between variables. The multiple linear regression model for downstream DOC flux with the lowest AIC score ($R^2 = 0.84$; $p<0.01$) that passed all selection criteria

retained seven variables, of which two were significant ($p<0.05$). Air temperature (0h, 72h) and rainfall (0h) were the best predictors of downstream DOC flux (Table 2.3). Air temperature (0h, 72h) showed a negative relationship with downstream DOC flux while rainfall showed a strong positive relationship (Table 2.3). The multiple linear regression model for upstream DOC with the lowest AIC score ($R^2 = 0.87$; $p<0.001$) that passed all selection criteria also retained seven variables, of which four were significant ($p<0.05$). Air temperature (0h, 72h) and rainfall (0h, 120h) again were the best predictors of upstream DOC flux (Table 2.3). Similar to the downstream model, air temperature had a negative relationship with DOC flux (Table 2.3), while time-of-sampling rainfall (0h) continued to have a strong positive relationship with DOC flux (Table 2.3). However 120h rainfall showed a negative relationship with DOC flux in this model (Table 2.3). Due to the nature of our sampling regime DOC concentrations during rainfall events were not always captured; the data suggest direct (0h) rainfall impacts are great, immediate, and transient, and may not have fully been captured in this study.

2.5 Discussion

2.5.1 Retrogressive thaw slumps and carbon delivery to streams of the Peel Plateau

In Eastern Siberia (Vonk et al., 2013a; Drake et al., 2015; Mann et al., 2015), Alaska (Balcarczyk et al., 2009; Abbott et al., 2014), and the Canadian High Arctic (Melville Island; Woods et al., 2011) the presence of permafrost slumping has been associated with significant increases in DOC concentration in recipient streams. This was not true on the Peel Plateau, where much greater variation in DOC concentration was observed among pristine stream sites, than change in DOC within streams as a result of slumping. When our study sites were assessed as a whole, using a paired-comparison approach, DOC concentrations were found to be slightly lower downstream of slumps than in upstream sites. However, paired comparisons of channelized slump runoff (our within sites) and un-impacted sites showed no consistent difference in DOC concentration between upstream sites and the slump-derived runoff being deposited into streams. Instead, DOC concentrations in slump runoff were either greater than, or less than, the comparison upstream site, depending on slump morphological characteristics (Fig.1.3; Table 2.1). The lack of a strong effect of slumping on DOC concentration and flux at these sites occurred despite the fact that slumping significantly affects the delivery of many biogeochemical constituents to streams within the Peel Plateau, a trend well-established for thermokarst features (Kokelj et al., 2002, 2005, 2013; Thompson et al., 2008; Keller et al., 2010; Malone et al., 2013). For example, conductivity

was, on average, 9.2-fold greater, while TSS was, on average, 446-fold greater, in waters draining slump sites when compared to upstream, un-impacted systems.

Downstream of slumps, an increase in indicators of slump activity (major ions, TSS), was accompanied by a modest decrease in DOC concentration. This effect may be due to a combination of low concentrations of DOC present in slump inflow (a dilution effect; particularly for slumps FM2, FM3, and FM4) and DOC sorption to suspended inorganic particles. Soils in the Peel Plateau are comprised of fine grained mineral till that is more receptive to DOC adsorption than other soil materials (Kothawala et al., 2009). For example, the mineral-rich sediment from the headwall of FM3 is classified as silty clay (64% silt, 29% clay, and 7% sand; Lacelle et al., 2013). The significantly elevated sediment load at within-slump and downstream locations provides the opportunity for increased adsorption (Fig. 2.2). DOC: TSS ratios also support this theory: while upstream sites have an average DOC: TSS ratio of 787.3, this ratio drops dramatically to 1.3 within slumps, and remains reduced downstream at 2.3.

Although DOC concentrations consistently declined downstream of slumps, this effect was much more modest than for lakes in the region, where slumping is associated with a strong negative correlation between conductivity and DOC. This is likely due to particle settling in lakes which enables scavenging, (removal from the water column) when significant inorganic particle inputs are present (Kokelj et al., 2005). This clear correlation between known indicators of slump activity (TSS, conductivity and major ion concentrations; Keller et al., 2010; Kokelj et al., 2013; Malone et al., 2013) and DOC concentration did not exist for stream sites on the Peel Plateau (Fig. 2.3). Overall, the significant influx of slump derived mineral materials on the Peel Plateau, coupled with low carbon content in regional soils, shows DOC mobilization from slumps in this region to differ substantially from trends found in other regions (Alaska and Siberia), where DOC increases alongside slump indicators after a disturbance (Vonk et al., 2013b; Abbott et al., 2014).

2.5.2 The effect of retrogressive thaw slumps on DOC composition

Despite the fact that DOC concentrations did not increase as a result of slumping, $SUVA_{254}$ and other absorbance metrics clearly indicate that slump-derived DOC is compositionally different than DOC at upstream locations; a trend seen in other thermokarst-affected regions (Abbott et al., 2014; Mann et al., 2015). Upstream waters had significantly higher $SUVA_{254}$ values of 3.75 (± 0.07) L mg C^{-1} m^{-1}, compared to downstream and within-slump values of 3.09 (±0.13) and 1.58 (±0.18) L mg C^{-1} m^{-1}, respectively (Fig. 2.2). Slope ratios (S_R) are a unit-less way to compare waters that undergo DOC chemical alterations during transit, and correlate well to the molecular weight of bulk DOC (Helms et al., 2008). S_R values of

approximately 0.70 are associated with fresh, terrestrial materials, and the average S_R value of Peel Plateau upstream waters was similar to these reported terrestrial values (0.74, ±0.005; Helms et al., 2008). Absorbance slopes, slope ratios and $SUVA_{254}$ values indicate that DOC derived from slump outflow is of lower molecular weight, and less aromatic, than upstream DOC (Weishaar & Aiken, 2003; Helms et al., 2008; Poulin et al., 2014). High $SUVA_{254}$ values accompanied by low S_R in upstream locations suggests that the impermeable permafrost layer upstream of slump disturbances constrains water flow to shallow, organic-rich flowpaths, and inhibits water contributions from deeper, groundwater sources (MacLean et al., 1999; Balcarczyk et al., 2009; O'Donnell et al., 2010; Mann et al., 2012). Within and downstream S_R values were greater than upstream values, indicating lower molecular weight DOC molecules, and a shift in composition from upstream waters.

$SUVA_{254}$ and S_R values for downstream and within-slump waters suggest that permafrost-derived carbon on the Peel Plateau is compositionally similar to permafrost carbon from other regions. For example, $SUVA_{254}$ values were much lower in active thaw slump sites on the North Slope of Alaska, compared to stabilized and undisturbed regions (Abbott et al., 2014), while in Siberia, older DOC in stream tributaries had lower $SUVA_{254}$ values compared to younger DOC in the Kolyma River mainstream (Neff et al., 2006). Comparatively, $SUVA_{254}$ values found in waters draining Siberian Yedoma are still not as low as values reported for our permafrost disturbances on the Peel Plateau. In comparisons between permafrost and active layer derived DOC, low molecular weight compounds, associated with low $SUVA_{254}$ values, have been found to be more easily degraded by bacteria (Abbott et al., 2014; Drake et al., 2015), suggesting that the DOC from Peel Plateau thaw slumps could have a high biolability. However, overall global relationships between $SUVA_{254}$ and DOC degradation are relatively weak (Weishaar & Aiken, 2003; Fellman et al., 2008).

Oxygen isotope data provide further evidence that permafrost thaw enables novel sources of water and solutes to be transported to fluvial systems on the Peel Plateau. The $\delta^{18}O$ signature of within slump waters values are similar to the Holocene-aged 'icy diamicton' values reported in Lacelle et al. (2013). These values are less depleted than those previously reported for ground ice present in thaw slumps (Lacelle et al., 2013), which suggests that our outflow samples are likely comprised of a mixture of Pleistocene-aged ground ice from beneath the thaw unconformity and Holocene-aged to modern sourced water, bringing with it DOC of variable composition, and different solute loads. In contrast, downstream and upstream $\delta^{18}O$ values were both similar to modern active layer values presented by Lacelle et al. (2013), demonstrating significant dilution and mixing after the merging of the slump

outflow and the upstream channel. $SUVA_{254}$ values plotted against $\delta^{18}O$ demonstrate more depleted samples found within the slump outflow are correlated with lower $SUVA_{254}$, suggesting older sourced waters could potentially be preferentially degraded within the ecosystem, warranting further research into thaw slump influence on DOC lability (Fig. 2.5).

2.5.3 Variation in the effects of slumping across the Peel Plateau landscape

One of the more noticeable trends in this study is the effect of slump age and structure on DOC concentration differences between within-slump and upstream sites, where slump structure refers to both the height of the headwall and the total area influenced by slumping. For example, larger slumps (FM4, FM2 and FM3) with deep headwalls display DOC concentrations that are lower at within-slump locations compared to upstream, unimpacted locations. At these sites, slumps access deeper layers comprised of mineral-rich tills that guide their interactions with DOC. The deep headwalls at these larger slump sites extend past the thaw unconformity, with $\delta^{18}O$ values indicating that older Pleistocene-aged permafrost is being accessed and transported.

In contrast, SD, the youngest and most shallow slump surveyed, displays a pattern differing significantly from the mega slumps described above. Within-slump $SUVA_{254}$ values are similar to, or slightly greater than, upstream and downstream values and this trend continues across all optical properties, indicating that the DOC composition is similar across upstream, downstream and within-slump sites at SD (Fig. 2.4). This is most likely due to the shallow headwall and recent establishment of SD (Table 1.1); therefore, while slump activity has exposed permafrost soils at this site, it has not yet accessed deeper, mineral rich layers with older sourced water and differing DOC composition (Fig 2.5). This is evidenced by the similarly enriched $\delta^{18}O$ values across all sampling locations for SD, which are all similar to the modern active layer value measured by Lacelle et al. (2013; Fig. 2.5). As a result, the effect of slumping at SD is more muted when compared to larger, older slumps in the region. The different age/size classes of slumps included in our study demonstrate how slumps and slump impacts develop over time, highlighting the need for a long term focus on thaw slump impacts on downstream ecosystems. The lack of correlation between DOC and slump indicators is potentially explained through the influence of slump age and activity on DOC, which contrasts with the more consistent influence of general permafrost thaw on slump indicators (Bowden et al., 2008; Abbott et al., 2014, 2015).

2.5.4 Environmental drivers of DOC flux

Air temperature and rainfall were the greatest factors influencing DOC mobilization from both un-impacted landscapes of the Peel Plateau, and slump sites downstream of slump impact (Table 2.2). Of

these environmental variables, air temperature showed a negative correlation with DOC flux while rainfall showed a positive correlation; DOC flux increased for both upstream and downstream locations after rainfall. However, increases in the downstream system were more moderate than anticipated, as slump features were expected to allow for more rapid mobilization of DOC compared to the landscape. This lack of response could potentially be attributed to dilution or increased adsorption to mineral particles, which can occur within seconds to minutes (Qualls & Haines, 1992). The negative correlation between DOC mobilization and temperature first appears to be counterintuitive as increasing temperatures in the Arctic are expected to exacerbate thermokarst development; however decreases in temperature are associated with precipitation events (Fig. 2.6), suggesting that precipitation is the primary driver of DOC mobilization in this region. These results are consistent with previous work on the Peel Plateau which found that precipitation was the main driver of slump headwall retreat, and that air temperature had a much smaller influence (Kokelj et al., 2015).

Results from other regions, however, show that other environmental variables also have the potential to drive slumping. For example, Grom & Pollard (2008) found that solar radiation was the most important regulator of ablation rates in Eureka Sound, where little annual precipitation occurs, demonstrating that retreat, ablation and solute runoff drivers are dependent on the local climate conditions which vary strongly by region. The temporal scale of the environmental measurements can also affect the ability to discern the role of environmental conditions in headwall ablation or retreat rate. Studies investigating microclimates and shorter timescales tend to find correlations between environmental variables and slump activity (Cogley & McCann, 1976; Lewkowicz, 1985, 1986, 1987; Burn & Lewkowicz, 1990; Lamoureux & Lafreniére, 2009; Wang et al., 2009; Kokelj et al., 2015) compared studies encompassing broader scale measurements (Lacelle et al., 2015).

In general, results from environmental correlation studies can help predict how slump-affected ecosystems will be influenced by climate change should observed climatic trends continue, especially increases in precipitation. Across Arctic regions, precipitation is expected to increase significantly in the future (Walsh et al., 2011) and this increase is already being observed on the Peel Plateau with a rise in the frequency and magnitude of precipitation events in the past decade (Kokelj et al., 2015). Knowledge of the factors driving DOC flux from thermokarst features and permafrost landscapes can provide information concerning future changes in ecosystem functioning. For example, increasing DOC is an increase in the food source for bacteria but can also decrease primary productivity through shading; both of these changes can lead to alterations in ecosystem functioning (Salonen & Hammar, 1986;

Tranvik, 1988; Hessen, 1992; Carpenter et al., 1998; Williamson et al., 1999; Hanson et al., 2003). At a broader scale, an increase in the input of organic carbon to the contemporary Arctic carbon cycle has the potential to influence climate change through increased mineralization rates and propagation of the permafrost carbon feedback cycle (Schuur et al., 2015; Vonk et al., 2015a; Abbott et al., 2016).

2.5.5 Dissolved carbon mobilization across diverse permafrost-affected landscapes

Across the pan-Arctic, carbon dynamics are influenced by numerous factors, including glaciation history, geology, soil composition, vegetation and thermokarst activity. As a result, the effect of permafrost thaw on DOC concentration and flux in streams will also be variable. For example, while DOC values found in this study are comparable to DOC values found in active thaw slumps in Alaska (Abbott et al., 2014, 2015), our average within-slump DOC concentration is 16 times lower than average DOC values found in Yedoma thaw streams in Siberia (Vonk et al., 2013a). Unlike both of these regions, where DOC in impacted streams was double or triple that of unimpacted DOC concentrations (Vonk et al., 2013a; Abbott et al., 2014; Larouche et al., 2015), DOC decreased between upstream and downstream sampling locations on the Peel Plateau. Thus, it seems clear that results from multiple regions are needed to understand change across the pan-Arctic. Reliance on few regional studies to quantify and map changing freshwater carbon dynamics for the entire Arctic can lead to over (or under-) estimations of carbon input to stream ecosystems, especially when applying values found in carbon-rich Yedoma regions to previously glaciated regions with deep, unweathered glacial tills and poor organic soil development. This study effectively demonstrates that across the pan-Arctic, we should expect large inter-regional variations in carbon flux to streams in response to permafrost thaw.

A focus on modelling efforts would be beneficial to enable more accurate predictions of how carbon delivery from terrestrial to aquatic systems will respond to climate change on a pan-Arctic scale. To be accurate, such models would need to incorporate information about geology and glaciation history, active layer depth and overall soil composition, permafrost extent, slump morphology, and environmental variables, especially precipitation and air temperature as these factors have been shown to influence both carbon dynamics and thermokarst development (Lewkowicz, 1986, 1987; Lewkowicz & Harris, 2005; Lacelle et al., 2010, 2015; Malone et al., 2013; Brooker et al., 2014; Kokelj et al., 2015). Lacelle et al. (2015) have brought to attention the fact that an understanding of regional-scale terrain controls on thaw slump initiation and development is needed before predictions can be made of the impacts of thermokarst disturbances. While research is being conducted to monitor the activity and growth of thaw slumps at regional scales (Brooker et al., 2014), and the impacts of slumps on fluvial

geochemistry at the watershed scale (Rudy et al., 2015), more research is needed before trends of thermokarst impacts on fluvial systems can be discussed at a circumpolar scale, as great variation in carbon response to thermokarst activity throughout Arctic regions has been observed.

2.6 Figures

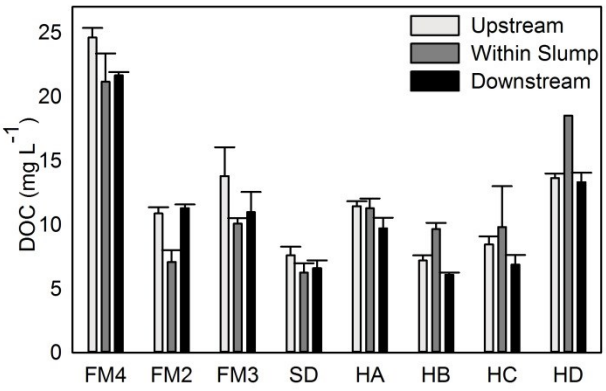

Figure 2.1 Dissolved organic carbon (DOC) concentrations across all sampling time periods for each retrogressive thaw slump. Bars represent replicates from an individual slump, sampled over three time periods between July and August, 2014; Period 1 was sampled early July; Period 2, late July; and Period 3, early August. Sites HA,HB,HC, and HD show averages for samples collected over a single time period (P2) and FM3 shows an average for samples collected over two times periods (P1 and P2). The remainder of the slumps show an average of all three sampling periods. Error bars represent standard error (*n* explained above).

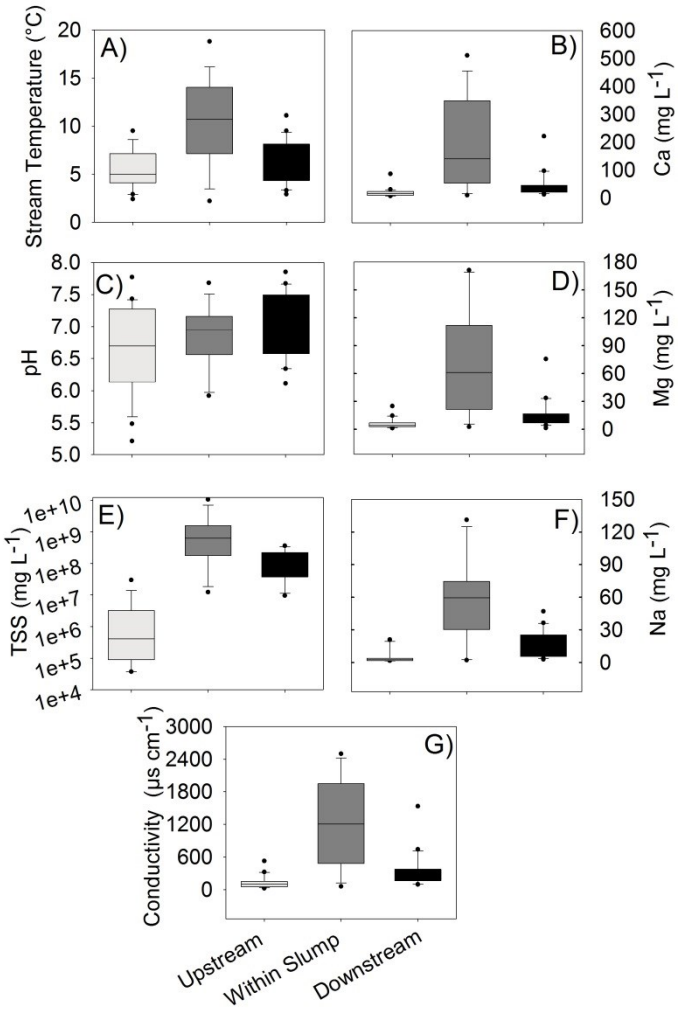

Figure 2.2 Active retrogressive thaw slump impacts on downstream geochemistry. Data points are averaged across all slumps and sampling periods. Significant differences were found between all sampling locations for all measures of stream geochemistry. Total suspended sediment is abbreviated as TSS in panel E.

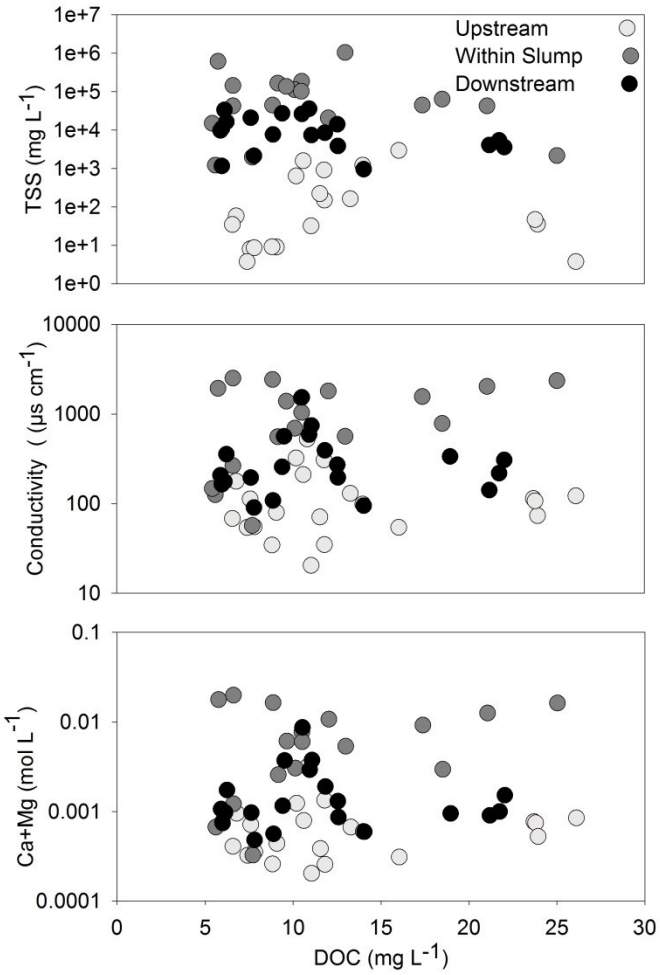

Figure 2.3 Dissolved organic carbon plotted against known indicators of slump activity and disturbance for the Peel Plateau. Data are compiled for all slumps; no clear trends are evident. Each point represents an individual sample point. Total suspended sediments is abbreviated as TSS in the top panel.

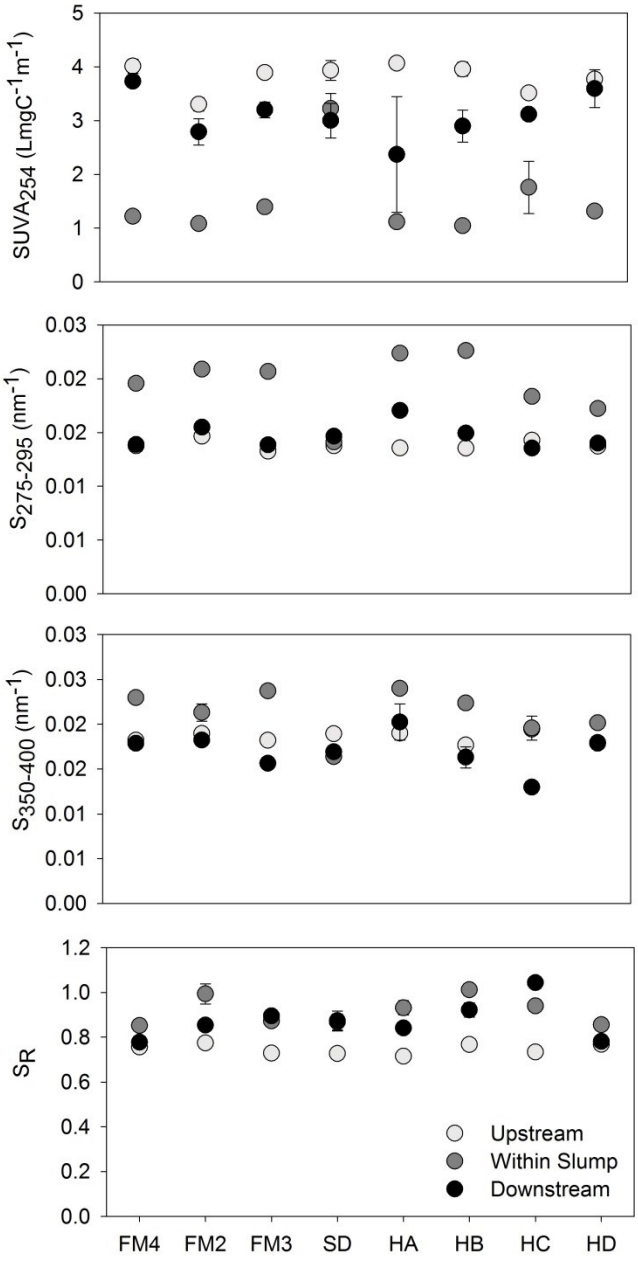

Figure 2.4 Optical properties across all sampling time periods for each retrogressive thaw slump. Each data point represents replicates from an individual slump sites. HA,HB,HC, and HD show averages for samples collected over a single time period (P2) and FM3 shows an average for samples collected over two times periods (P1 and P2). The remainder of the slumps show an average of all three sampling periods. Error bars represent standard error, with *n* as described above.

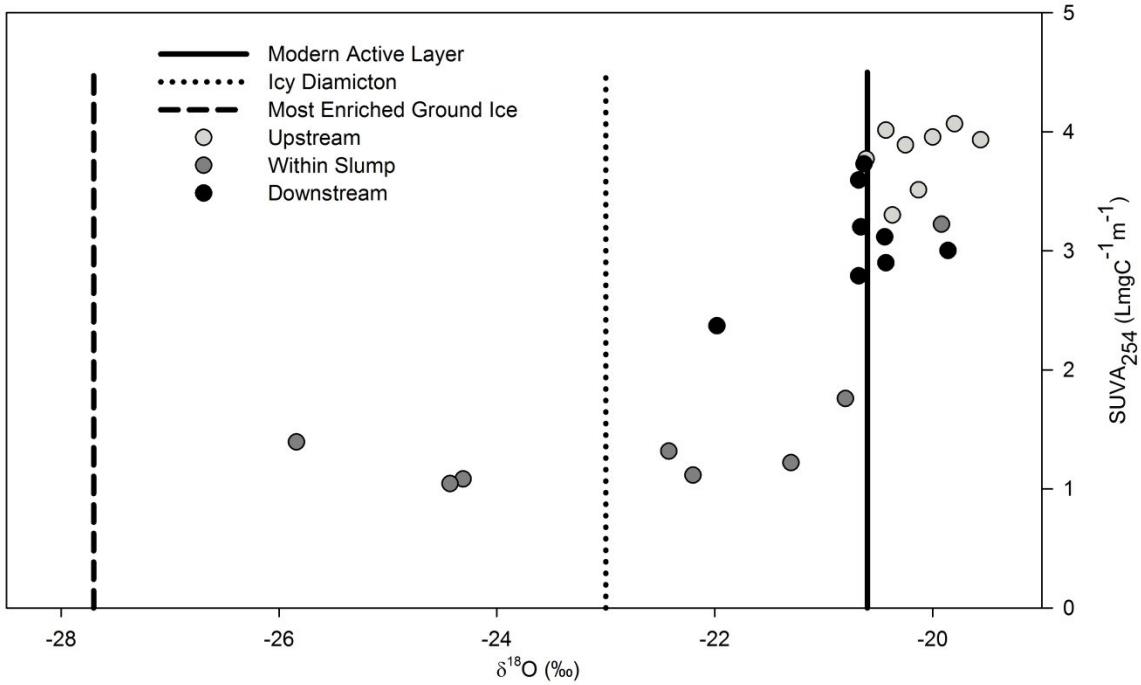

Figure 2.5 Oxygen isotope data ($\delta^{18}O$ ‰) plotted against ($SUVA_{254}$; L mg $C^{-1}m^{-1}$) to demonstrate the decrease in $SUVA_{254}$ with an increase in the age of the source water. References $\delta^{18}O$ values are taken from Lacelle et al. (2013). The modern active layer is equivalent ot the meteoric water line, icy diamicton is has been aged to be Holocene era, the most enriched ground ice value is the highest isotopic value for Pleistocene-aged ground ice found for this region (Lacelle et al., 2013).

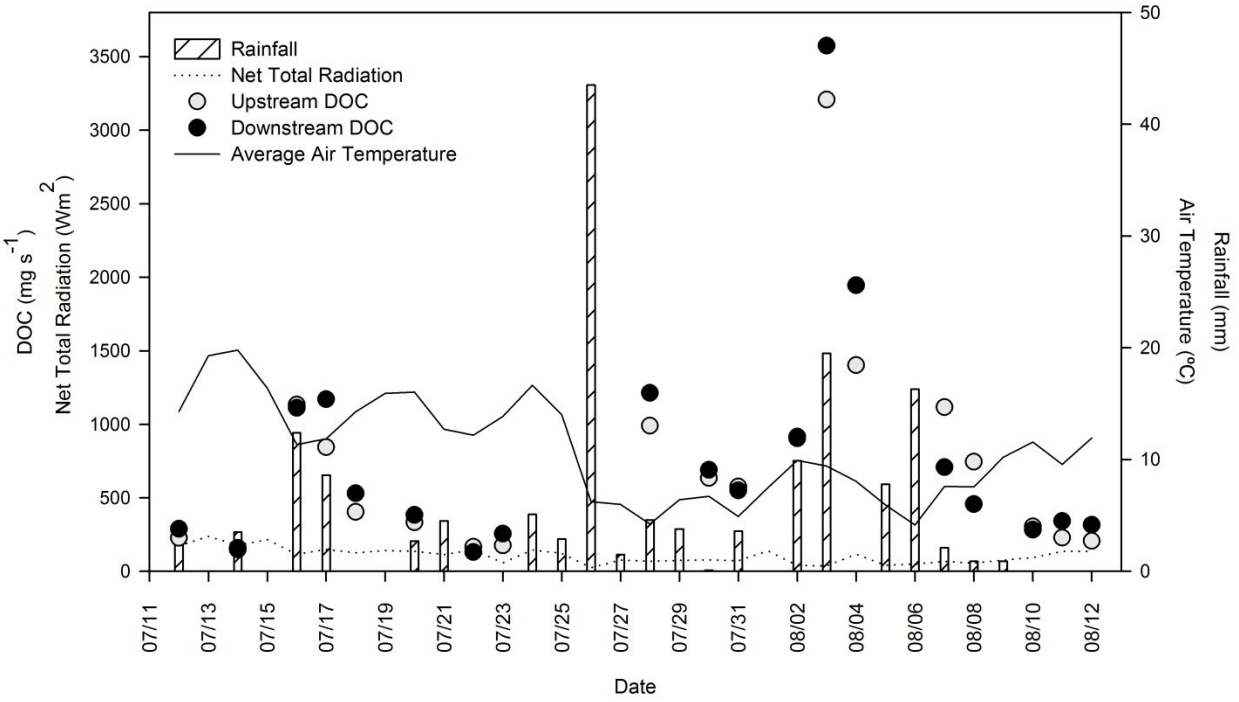

Figure 2.6 Environmental conditions (solar radiation, precipitation and average air temperature) and dissolved organic carbon (DOC) flux upstream and downstream of slump FM3 across a month-long sampling period (July 12-August 12, 2014). Multiple linear regressions were run to determine which variables influence DOC flux in thaw slumps, present (0h) and temporally shifted (48, 72 and 120 hour) data were used. Air temperature (0h, 72h) and rainfall (0h) showed the strongest correlation with downstream DOC flux. Air temperature (0h, 72h) and rainfall (0h, 120h) showed the strongest correlation with upstream DOC flux.

2.7 Tables

Table 2.1 Known slump characteristics for eight retrogressive thaw slumps sampled during the 2014 field season on the Peel Plateau, NWT, Canada.

Slump	Latitude	Longitude	Area (ha)	Headwall Height (m)
FM4	67 16.679	-135 09.573		16 to 20*
FM2	67 15.462	-135 14.216	48[2]	25 [1]
FM3	67 15.100	-135 16.270	10[2]	10 [1]
SD	67 10.818	-135 43.630		2 to 4*
HA	67 09.057	-135 41.121		10 to 15*
HB	67 14.397	-135 49.167	14[2]	10 to 15*
HC	67 19.564	-135 54.902		10 to 15*
HD	67 24.025	-135 20.048		10 to 15*
Weather Station	67 14.756	-135 12.920		

[1] (Kokelj et al., 2015)

[2] (Lacelle et al., 2015)

* Estimations by field crews over 2014 and 2015 field seasons.

Table 2.2 Summary of statistical results from paired t-tests and Wilcoxon signed rank sum tests for site characteristics. When data meet the assumption of normality a paired t-test was used to evaluate the data, when the assumption of normality was not met a Wilcoxon signed rank test was used.

	Paired t-test		Wilcoxon signed rank test		p-value
	df	t-value	N	W	
DOC (mg L^{-1})					
U-W			18	48	0.108
U-D			19	15	**0.001**
Ca (mg L^{-1})					
U-W			18	0	**<0.001**
U-D			21	1	**<0.001**
Mg (mg L^{-1})					
U-W			18	0	**<0.001**
U-D			21	8	**<0.001**
Na (mg L^{-1})					
U-W			18	0	**<0.001**
U-D			21	1	**<0.001**
Cl (mg L^{-1})					
U-W			12	0	**0.003**
U-D			17	16	**0.004**
Conductivity (µs cm^{-1})					
U-W			18	0	**<0.001**
U-D			21	1	**<0.001**
TSS (mg L^{-1})					
U-W			17	0	**<0.001**
U-D			18	1	**<0.001**
pH					
U-W	17	-1.60			0.128
U-D	20	-3.94			**<0.001**
Stream Temperature (°C)					
U-W	17	-4.61			**<0.001**
U-D	20	-3.12			**0.006**
$SUVA_{254}$ (L mg $C^{-1}m^{-1}$)					
U-W			18	0	**<0.001**
U-D	19	5.13			**<0.001**
S_{275} (nm^{-1})					
U-W			19	0	**<0.001**
U-D			20	29	**0.003**
S_{350} (nm^{-1})					
U-W			19	23	**<0.002**
U-D	19	2.61			**<0.017**
S_R					
U-W			19	0	**<0.001**
U-D			20	0	**<0.001**
DOC Flux (mg L^{-1})					
U-D			19	53	0.096

Table 2.3 Results from the multiple linear regressions between upstream and downstream DOC flux and environmental/ situational conditions (downstream: R^2=0.84, $F_{7,11}$=8.25, p-value= 0.001; upstream: R^2=0.87, $F_{7,11}$=10.79, p-value<0.001). NS represents variables that were not significant, as determined by the regression analysis;, N/A represents variables that were not run in individual analyses.

	Downstream DOC flux			Upstream DOC flux		
Coefficient	Estimate	t-value	p-value	Estimate	t-value	p-value
Average Air Temperature (°C)						
0 h	-67.08	-1.685	**0.014**	-115.96	-3.286	**0.007**
48 h	NS	NS	NS	56.32	1.534	0.153
72 h	-95.15	-2.594	**0.025**	-94.17	-2.717	**0.020**
120 h	NS	NS	NS	NS	NS	NS
Rainfall (mm)						
0h	116.13	5.411	**<0.001**	105.47	6.039	**<0.001**
48h	NS	NS	NS	NS	NS	NS
72h	NS	NS	NS	NS	NS	NS
120h	-23.94	-1.970	0.075	-24.15	-2.529	**0.028**
Average net radiation (W m^{-2})						
0h	4.96	1.286	0.225	NS	NS	NS
48h	NS	NS	NS	NS	NS	NS
72h	5.58	1.545	0.151	4.04	1.563	0.146
120h	NS	NS	NS	NS	NS	NS
Total suspended sediment (mg L^{-1})						
Downstream	-0.02	-2.102	0.059	N/A	N/A	N/A
Upstream	N/A	N/A	N/A	-0.32	-1.626	0.132

3.0 Unique trends in the biodegradability of dissolved organic carbon mobilized from retrogressive thaw slumps on the Peel Plateau, NWT, Canada

3.1 Introduction

As the Arctic warms (Walsh et al., 2011; IPCC, 2014), the rate of permafrost thaw continues to accelerate across Arctic landscapes (Smith et al., 2005; Jorgenson et al., 2010; Romanovsky et al., 2010; IPCC, 2014). In regions with ice-rich permafrost, permafrost thaw leads to the formation of thermokarst features (Kokelj & Jorgenson, 2013). Where thermokarst occurs over hilly terrain, these erosive features mobilize sediments, nutrients and carbon from below the active layer and deep in the permafrost (Bowden et al., 2008; Schuur et al., 2008; Grosse et al., 2011; Kokelj et al., 2013; Malone et al., 2013). The effect of these processes across the Arctic is anticipated to be significant; projections estimate degradation rates of 80% of near surface permafrost by 2100 (Slater & Lawrence, 2013), with 5.5 x 10^6 km^2 of Arctic landscapes predicted to be impacted by thermokarst features (Abbott et al., 2014).

There is a large pool of organic carbon stored in permafrost soils; global permafrost carbon stocks are estimated at 1670 Pg; twice that of the atmospheric carbon pool (Hugelius et al., 2014). Estimated carbon pools for the western Canadian Arctic are 50-100 kg m^{-2}, although these estimates contain large uncertainty ranges as data for this region are scarce (Hugelius et al., 2013, 2014). With permafrost degradation, more than 220 Pg of carbon is predicted to be lost from global permafrost soils by 2100 (Schaefer et al., 2011; Schuur et al., 2013). While some of this carbon is delivered to the Arctic Ocean and its surrounding basins, most is expected to be processed or buried in terrestrial aquatic systems (McGuire et al., 2010; Aufdenkampe et al., 2011; Spencer et al., 2015; Abbott et al., 2016). Despite the clear ecological and carbon cycle impacts of increased delivery of organic carbon to aquatic systems, there is a lack of consensus in the scientific community as to how carbon cycling in the Arctic will be altered with increasing permafrost thaw (Laudon et al., 2012; Hinzman et al., 2013; Abbott et al., 2016). However, there is overwhelming agreement that there will be increased coupling of carbon and hydrological cycles in the Arctic, and that this increased coupling will lead to alterations in these cycles (Schuur et al., 2008; Aufdenkampe et al., 2011; Vonk et al., 2015b). The permafrost carbon feedback

cycle is also in play in Arctic regions, and is expected to have a significant impact on climate (Schuur et al., 2008, 2013; Schaefer et al., 2011). The permafrost carbon feedback is a positive feedback cycle whereby the increase in global temperatures prompts the thawing of permafrost and the release of carbon, which in turn degrades; releasing greenhouse gases further increasing temperatures (MacDougall et al., 2012; Schneider Von Deimling et al., 2012; Schuur et al., 2015).

Dissolved organic carbon (DOC) has been the main focus of studies exploring the fate of organic carbon transported to aquatic systems as a result of permafrost thaw. DOC is the most prominent form of organic carbon in Arctic riverine systems and is the primary substrate in microbial metabolism as it is easily transported across cell membranes (Battin et al., 2008; Frey & McClelland, 2009; Spencer et al., 2015). One increasingly common method to explore the fate of DOC in aquatic ecosystems is through the use of incubation experiments that measure biodegradable DOC (BDOC), or the amount of DOC loss over a specified time period, in incubations that are filtered to exclude all particles larger than bacteria. Quantification of DOC metabolism, and its mineralization to CO_2, is important as this carbon provides a novel input to carbon cycles, and is a key regulator of carbon release to the atmosphere as a result of permafrost thaw (Holmes et al., 2008; Mann et al., 2012; Wickland et al., 2012; Abbott et al., 2014; Vonk et al., 2015b). One of the main controls on BDOC is the composition of DOC that becomes available for processing (Kalbitz et al., 2003). Permafrost DOC is expected to have a different composition compared to DOC derived from surficial flowpaths (Neff et al., 2006; Spencer et al., 2008; Mann et al., 2012; O'Donnell et al., 2012). However, permafrost DOC concentrations, degradation and variability trends are still widely unknown (Wickland et al., 2012; Abbott et al., 2016).

The objectives of this study were to determine the degradability of DOC mobilized by thaw slumps in the western Canadian Arctic, and to determine factors that drive BDOC in this region through manipulated incubations and an exploration of temperature and nutrient controls on BDOC. This work was undertaken in a region where permafrost slumping exposes deep mineral soils deposited as glacial till following the last glacial maximum. As a result, the permafrost soils in this region differ substantially from the organic-rich, often yedoma-origin soils where much of the previous work on biological lability of permafrost-origin DOC has occurred (Vonk et al., 2013a, 2013b; Drake et al., 2015). These differences in landscape characteristics are predicted to decrease the magnitude of degradation in permafrost carbon; however permafrost degradation rates are expected to be greater than regional unimpacted carbon degradation. In some laboratory incubations, the concept of 'hydrological biolability', which is

the potential biodegradability of DOC within the constraints of the environment experienced, is used to structure incubation conditions. These constraints include nutrient concentrations, residence times and temperature (Vonk et al., 2013a). Carbon dynamics data are scare for most Arctic regions but especially the Canadian Arctic. To our knowledge this study is the first DOC degradation experiment on thermokarst carbon in the western Canadian Arctic.

3.2 Study site

Incubation experiments were conducted on samples from eight thaw slumps located across the Peel Plateau; situated in the eastern foothills of the Richardson Mountains, NWT in a continuous permafrost zone. Lower Cretaceous marine shale from the Arctic River Formation forms the bedrock for this region (Norris, 1984) and is overlain by siltstone and Late Pleistocene glacial, glacio-fluvial and glacio-lacustrine sediments (Duk-Rodkin & Hughes, 1992); the region has a shallow organic layer. Regional ground ice has been dated to the late Pleistocene epoch while upper layers of the soil profile, delineated by a thaw unconformity, have been aged as early Holocene (Lacelle et al., 2013). The mineral rich soil present in the western Canadian Arctic sharply contrast with that of Yedoma soils found throughout much of Beringia, where a third of organic carbon stored in permafrost regions is estimated to reside (Tarnocai et al., 2009; Vonk et al., 2013b). Estimates of the soil organic carbon content for the Peel Plateau are estimated to range from 10-50 kg m^{-2} (Tarnocai et al., 2009) to 75-100 kg m^{-2} (Hugelius et al., 2014) for the top three metres of soil.

The Peel Plateau has numerous slump features, with 212 thaw slumps currently mapped, 89% of which are active (Lacelle et al., 2015). Slump size ranges from small, newly developing slumps, which are relatively numerous, to those greater than 20 ha, which are rare (<5% prevalence). Slumps sampled in this study range across a variety of sizes and ages. The regional climate is typical of subarctic regions with long, cold winters and short, cool summers. A warming trend of 0.77 ^{o}C per decade since 1970 has been recorded; primarily observed in in the winter months (Burn & Kokelj, 2009). Mean annual air temperature (1981-2010) at the Fort McPherson weather station is -7.3^{o}C (Environment Canada, 2015). Annual cumulative rainfall (1981-2010) averages 145.9 mm (Environment Canada, 2015). Comparatively, 2014 was wetter and cooler than these long term averages (see Chapter 2).

3.3 Methods

3.3.1 Slump site selection

Across the Peel Plateau eight thaw slump sites were selected as part of this study (Fig. 1.1). Over the two month sampling season, three slumps were sampled three times and five were accessed twice. Slumps selected for sampling possessed a debris tongue that extended to the valley bottom and directly impacted a stream system. Three discrete locations at each slump were sampled: upstream, within-slump, and downstream of slump influence (Fig. 1.2). Upstream sites are pristine and uninfluenced by any other disturbances and connect with the slump flow path further downstream. Within-slump sites were chosen to provide a channelized flow within the main body of the disturbance, at the start of the debris tongue. The confluence of the upstream flow and all within-slump runoff paths was termed the downstream site and is representative of how slumps impact aquatic ecosystems across the landscape.

Slumps are incredibly diverse, therefore a general classification of the slumps is difficult (Table 1.1; Fig. 1.2). Slumps FM4, FM2, and FM3, are classified as 'mega slumps' which are characterised by areas greater than 5 ha and a headwall greater than four metres in height (Kokelj et al., 2013, 2015). FM4 is the largest of the thaw slumps in area and has a headwall approximately 20 m in height; the majority the slump is stabilized, and it therefore has a small outflow, long, dry debris tongue and significant revegetation. FM2 is considered one of the largest active slumps in the region, with a headwall approximately 25-30 m high and several hectares of slump activity. Slump FM3 has an area of approximately 10 ha and a headwall of approximately 10 m in height (Kokelj et al., 2015; Lacelle et al., 2015). Headwall stratigraphy conducted by Lacelle et al. (2013) at FM3 described an upper layer comprised of an icy diamicton that is Holocene aged (7890 $\pm$ 250 ^{14}Cyr BP) , formed by the Holocene warming, which lies above a thaw unconformity that covers Pleistocene-aged ground ice (18,100 $\pm$ 60 ^{14}Cyr BP). FM2 and FM3 geochemistry and geomorphology are well outlined in Malone et al. (2013). SD is the smallest and youngest slump in this study, with a headwall of 2-4 m and a length of approximately 20m, with no defined debris tongue. Slumps FM4, FM2, FM3 and SD were all accessed on foot from the Dempster Highway. Slumps HA, HB, HC, and HD are much more similar in age and size, and were accessed via helicopter. All helicopter accessed slumps are well established, active thaw slumps with headwalls of approximately 10-15 m and well-defined debris tongues (Fig. 1.2) and are less studied than the highway accessible sites.

3.3.2 Sampling

Samples were collected during three distinct time periods: Period 1 (early July; all eight slumps accessed); Period 2 (late July; all eight slumps accessed); and Period 3 (early/mid-August; FM2, FM4 and SD accessed). During the first time period, all three sampling locations (upstream, within-slump and downstream) were sampled at each slump; subsequent sampling occurred only at upstream and within slump locations. In addition to samples to be used for incubation experiments, $\delta^{18}O$ samples were collected directly from streams into an acid washed 40 mL HDPE bottles with no headspace and were then sealed and refrigerated until analysis. All other water samples were obtained from directly below the stream surface into 1 L acid washed HDPE bottles and placed in chilled, dark conditions for 24 hours to allow settling of suspended sediments.

Sample water was filtered with pre-combusted (475°C, 4 hours) Whatman GF/F filters (0.7 µm pore size). To set up BDOC incubation experiments, 30 mL of GF/F-filtered water from upstream, within-slump, or downstream sites was transferred into 40 mL acid washed, pre-combusted glass bottles and inoculated with 3 mL of upstream water filtered through pre-combusted (475°C, 4 hours) Whatman GF/C filters (1.2 µm pore size) to introduce indigenous microbial communities (a 10% addition). Samples were then either immediately placed into an incubation environment or terminated for T_0 measurements (see below). The remainder of the filtered sample water was then transferred into 60 mL acid washed HDPE bottles for later analysis of absorbance, total dissolved phosphorous (TDP), and total dissolved nitrogen (TDN) and refrigerated until analysis (see below). This information, along with $\delta^{18}O$ data, were used to understand controls on DOC degradation.

3.3.3 Experimental incubation design

Incubations for DOC degradation were set up in triplicate under three different incubation conditions (Table 3.1), following the methodology of Vonk et al. (2015). The 28 day, 20°C (control) incubations was designed as baseline standard for comparisons with previous studies and measures complete DOC degradation. The in-situ temperature treatments, Env and Env+N, ran for 28 days at 6.4 °C, and were designed to measure hydrological biolability through replicating environmental conditions. The Env+N treatment contained a nutrient addition that mimics maximum nutrient concentrations of nitrate, phosphate and ammonium in the Beaufort Sea (Table 3.2; Simpson et al., 2008) and is considered the environmental maximum for degradation potential. Incubations were set up in either an incubator (20°C treatment) or a lab refrigerator that was intended to mimic in-stream temperatures (Env treatments). Temperatures were monitored throughout all incubations.

To avoid anoxic conditions sample caps were applied loosely. Samples were refiltered with pre-combusted (475°C, 4 hours) Whatman GF/F filters at the termination of the incubation and acidified with hydrochloric acid (1 µL mL^{-1}) to prevent any further degradation, following Vonk et al. (2015). Samples were kept refrigerated until analysis for DOC concentration. Re-filtration of the samples means that the DOC loss measured is a result of both DOC mineralization by microbes and incorporation into microbial biomass, which is typically minor (Vonk et al., 2015b). The absolute change in DOC loss (mg L^{-1}; ΔDOC) was calculated by subtracting the $T_{incubation}$ DOC concentration from the T_0 DOC concentration. Biodegradable DOC (BDOC) was calculated as percent loss over incubation time, calculated by dividing ΔDOC (T_0/ $T_{incubation}$) by the T_0 DOC concentration, and multiplying by 100.

3.3.4 Laboratory analyses

In-situ nutrients (TDP and TDN) were analyzed using Flow Injection Analysis on a Lachat QuikChem 8500 FIA automated ion analyzer. A Picarro liquid water isotope analyzer was used to measure stable water isotope samples at the University of Alberta (precision: ± 0.2%). DOC was measured on a Shimadzu TOC-V analyzer; and calculated as the mean of the best 3 of 5 injections with a coefficient of variance of <2%. SUVA and S_R were calculated from UV visible spectra data from 250-750 nm measured on a Genesys 10 UV-Vis spectrophotometer following the methodology in Chapter 2. Slope ratios (S_R) were calculated by dividing the calculated slope values of $S_{275-295}$ by $S_{350-400}$.

3.3.5 Data treatment and statistical analyses

Data from helicopter accessed slumps (HA, HB, HC, and HD) collected during the first sampling period were also eliminated as the methodology changed significantly after this sampling day and therefore the results cannot be compared with confidence to those from the other sampling periods.

Statistical analyses were completed in R version 3.1.3 (R Core Team, 2015). R packages used included 'car' (Fox & Weisberg, 2011), 'nortest' (Gross & Ligges, 2015) 'nlme' (Pinheiro et al., 2015), 'lmtest' (Zeileis & Hothorn, 2002), and 'zoo' (Zeileis & Grothendieck, 2005). Wilcoxon Signed Rank Tests were run on paired upstream-within and upstream-downstream DOC concentration data. To take a statistically conservative approach the Dunn-Šidák method was applied to adjust alpha levels to ensure Type 1 errors did not occur as a result of multiple comparisons ($\alpha = 0.0253$).

The effect of slump (FM2, FM3, FM4, SD, HA, HB, HC and HD) and location (upstream, within slump and downstream) on BDOC (% loss), was evaluated using two-way ANOVAs. ANOVAs were separated by period (early season (1), mid-season (2), and later season (3)) and treatment (control, Env and Env+N),

due to an unbalanced design. When sample sizes for the contrasts were unequal they were corrected with harmonic means (Zar, 2010). All ANOVAs passed tests for normality and heteroscedasticity. When the two way interaction was significant, simple effects were used to test the effect of location within each slump (Keppel & Wickens, 2004). All significant simple effects were followed by simple contrasts (Keppel & Wickens, 2004) for the first period to show the direction of the effect, where three locations were sampled.

Multiple linear regressions were conducted to assess how differences in water chemistry (TDN and TDP), DOC composition (SUVA $_{254}$, S_R, $S_{275-295}$ and $S_{350-400}$), water source ($\delta^{18}O$), incubation settings (temperature and nutrient addition) and sampling regime (Julian Date) influence DOC degradation. Optical properties (SUVA $_{254}$, S_R, $S_{275-295}$ and $S_{350-400}$), demonstrated variance inflation factors (VIF) greater than 10 and significant Durbin Watson test results (indicative of correlated variables; Durbin & Watson, 1950; Hair et al., 1995), therefore the optical metric that displayed the highest correlation with DOC loss in the model outcome (S_R) was retained as an input for subsequent model selection and the remaining optical measurements were discarded from the model. AIC values were used to determine the best model fit (Burnham & Anderson, 2002). Models were tested for serial correlation using the auto-correlation function (ACF) in R and residuals were examined (Zuur et al., 2009). Residuals showed correlation, which is predictable as many of the values were applied across slumps. In an attempt to correct this, auto-regressive moving average (ARMA) models were run to determine the influence of the auto-correlation (Zuur et al., 2009). However, AIC values did not improve so corrections were not applied to the final model; note that this final model had VIF less than 10. This method is deemed acceptable as the model is structured in a reasonable, meaningful and functional way (Zuur et al., 2009).

One-way ANOVAs were run to determine the effect of temperature (as Q_{10}) and incubation nutrient additions on DOC loss. Q_{10} is the increase in a rate, in this case the increase in percent DOC loss, which occurs with a 10^{o}C increase in temperature. Significant results were followed by Tukey's post hoc tests. When calculating rates for nutrient impacts and Q_{10}, negative values were eliminated to adhere to mathematical conventions; these eliminations did not impact statistical results. Finally, regressions were run between S_R and BDOC (%) and $SUVA_{254}$ and BDOC (%) to determine the influence optical properties have on the DOC degradation.

3.4 Results

3.4.1 Experimental conditions, and biodegradable DOC trends

In situ stream temperatures measured at slump FM3 over the course of the field season showed an average temperature for upstream sites of 6.8 ± 0.09 °C, and an average for downstream sites of 7.9 ± 0.12 °C. The monitored environmental incubation temperatures averaged 6.4 ± 0.04 °C; thus the Env and Env+N incubation temperature of 6.4 ± 0.04 were reflective of temperatures in streams over the course of the incubation period.

In contrast to other Arctic regions, concentrations of DOC in waters draining slumps of the Peel Plateau were not significantly different from concentrations found immediately upstream of slumps (W=31, p=0.107), while downstream DOC declined as a result of slumping (W=15, p=<0.01). The overall range of DOC concentrations found at Peel Plateau slump sites is shown in Fig. 3.1. Despite this lack of strong effect of slumping on DOC concentration, however, DOC degradation rates were clearly elevated in waters draining slumps, when compared to upstream and downstream locations. ΔDOC showed a consistent trend across all incubations, with the greatest loss of DOC occurring for water from within-slump sites (control: 1.77 mg L^{-1} ± 0.34; Env: 1.10 mg L^{-1} ± 0.20; Env+N: 1.94 mg L^{-1} ± 0.33), followed by downstream incubations (control: 0.61 mg L^{-1} ± 0.07; Env: 0.46 mg L^{-1} ± 0.07; Env+N: 0.49 mg L^{-1} ± 0.12). Upstream incubations displayed the lowest absolute DOC loss (control: 0.36 mg L^{-1} ± 0.07; Env: 0.24 mg L^{-1} ± 0.05; Env+N: 0.25 mg L^{-1} ± 0.05; Fig 3.2).

Differences in DOC degradation between slump-influenced and un-influenced sites were particularly striking when examined as the percent loss of DOC over the incubation treatment (BDOC). Similar to ΔDOC, BDOC showed relatively consistent patterns across all incubations. For the control incubation average within-slump BDOC was greatest across all time periods, (Period 1: within-slump: 9.44 % loss ± 0.97, downstream: 5.7 % loss ± 0.95, upstream: 3.05 % loss ± 0.57; Period 2: within-slump: 14.22 % loss ± 1.62, upstream: 1.00 % loss ± 0.46; Period 3: within-slump: 7.21 % loss ± 0.96, upstream: 5.18 % loss ± 0.70). In general, within-slump BDOC degradation was greater at all slump sites than both downstream and upstream DOC losses, except in the case of SD, where downstream BDOC was greatest (Fig 3.3).

A series of two-way ANOVAs, coupled with the analysis of simple effects where interactions were significant, were conducted to parse out statistical differences in BDOC between upstream, within-slump and downstream locations. In the first period, BDOC was typically greater within slumps compared to upstream locations, while upstream-downstream differences were typically not significant.

These patterns were similar across all incubations (Fig. 3.3; Tables 3.3 and 3.4). In one instance (SD, Env) downstream BDOC was greatest, followed by within-slump and then upstream DOC loss. There was only one instance where simple contrasts showed no statistical differences between the sampling locations even though simple effects were significant at this site (SC, control, Period 1; Table 3.4).

In the second sampling period, within-slump DOC degradation rates were consistently greater than upstream degradation rates; this was true across all sites and incubation treatments (Fig. 3.3; Tables 3.3 and 3.4). In the third sampling period slump: location interactions were non-significant for the control and Env incubations (Table 3.3), and thus an analysis of simple interactions was not required. In the control incubation, the effect of location was significant, indicating that within-slump BDOC was greater than upstream BDOC across all sites (Fig. 3.3, Table 3.3). In the Env incubation, the effect of location was not significant, indicating there was no statistical difference between within-slump and upstream sites. For the Env+N incubation, simple effects determined that within-slump BDOC was greater than upstream DOC loss in two-thirds of the slumps sampled (Table 3.4).

3.4.2 Drivers of DOC degradation

3.4.2.1 Experimental drivers of DOC degradation

The direct manipulation of temperature and nutrients in the experimental incubations enabled a more detailed analysis of their effects of these factors on BDOC. To examine the effect of temperature on DOC loss rates, Q_{10} values were calculated using control (average 19.5 ºC) and Env (average 6.4 ºC) incubations. When Q_{10} data were compiled across slumps, upstream locations had the largest Q_{10} values (1.90 ± 0.26), followed by within-slump (1.49 ± 0.11) and then downstream locations (1.36 ± 0.21; Fig. 3.5). However, there was no significant difference in Q_{10} values between sampling locations ($F_{2,28}$=1.584, p=0.223). Absolute differences in the effect of temperature on DOC degradation were also calculated, as the difference in absolute DOC loss (ΔDOC) between the control and Env treatments. These calculations showed temperature to have the greatest absolute effect on DOC degradation for incubations with within-slump waters (0.72 mg $L^{-1} \pm 0.28$), followed by upstream waters (0.18 mg $L^{-1} \pm 0.06$) and downstream again showing the smallest temperature effect (0.15 mg $L^{-1} \pm 0.12$). Despite the large absolute difference in temperature effect between the within-slump and in-stream sites, large ranges in variation led to no significant differences in ΔDOC between locations ($F_{2,28}$=2.119, p=0.139).

The impact of nutrient additions on DOC loss rates were examined by comparing DOC loss in the Env and Env+N incubation treatments. The proportional effect of nutrient addition on DOC loss shows no

statistical differences between locations ($F_{2,26}$=0.561, p= 0.578; Fig. 3.6). While within-slump waters show the greatest absolute increase in DOC degradation as a result of nutrient addition, this increase is caused by the greater degradation capability of these waters, rather than a greater proportional increase in degradation as a result of nutrient amendments. Nutrient additions were shown to increase absolute DOC loss (ΔDOC) with slumping ($F_{2,26}$=5.487, p= 0.010). Tukey post hoc tests showed significant difference between within-slump and upstream locations (means difference= 0.882, p<0.01). The effect of nutrient additions on ΔDOC was greatest for within-slump waters (0.90 mg $L^{-1} \pm$ 0.26), followed by downstream waters (0.17 mg $L^{-1} \pm$ 0.02) and then upstream waters showing minimal increases with nutrient additions (0.02 mg $L^{-1} \pm$ 0.06).

3.4.2.2 Overall drivers of DOC degradation

An examination of the in situ and experimental variables driving variations in BDOC was conducted for the control incubation, to determine overall controls on BDOC. The multiple linear regression model with the lowest AIC score (R^2 = 0.55; p<0.001) that passed all selection criteria retained six variables, of which all were significant (Table 3.5). $\delta^{18}O$, TDN (μg L^{-1} N), slope ratio (S_R), incubation temperature (ºC), nutrient addition (presence/absence) and Julian Date were all significant predictors of DOC lability (Table 3.5). Of these variables the strongest predictors (p<0.001) were S_R, TDN, incubation temperature (ºC), and nutrient addition, two of which were incubation manipulations; all significant variables, except $\delta^{18}O$, were positively related to BDOC.

DOC percent loss was plotted against S_R and $\delta^{18}O$ for the control incubation to examine their significant influence on DOC degradation rates as determined by the regression analysis (Figs. 3.5 and 3.6). Across all sampling periods, the $\delta^{18}O$ -BDOC relationship shows a clumping of the upstream and downstream slump points at low DOC loss rates, with $\delta^{18}O$ values that hover around meteoric levels, while the within-slump points show higher DOC losses and more depleted $\delta^{18}O$ signatures, and greater variation between sites. Within- slump $\delta^{18}O$ values are similar to recorded (Pleistocene-origin) ground ice and (Holocene-origin) icy diamicton $\delta^{18}O$ levels. Within-slump and downstream relationships between S_R and $\delta^{18}O$ are similar, and continue to be separate from upstream values. As a general trend, higher S_R, indicative of lower molecular weight, is associated with greater DOC loss, especially for the second sampling period (R^2=0.57, p=<0.001). For the control incubation, regression analyses were performed on $SUVA_{254}$ data compiled across slump and time periods and correlated with BDOC and showed strong correlations ($SUVA_{254}$:R^2= 0.67, p=<0.001).

3.5 Discussion

3.5.1 Permafrost DOC degradation across circum-Arctic regions

Across the eight studied slump sites, DOC concentrations were either unchanged (within-slump), or decreased slightly (downstream) in comparison to concentrations upstream of slumps (Fig. 3.1; Chapter 2). In contrast to this relatively modest effect of slumping on DOC concentrations of the Peel Plateau, DOC biodegradability was significantly elevated in slump-affected waters. This was true across the three time periods studied, and occurred irrespective of nutrient addition, or changes in incubation temperature. Thus, while the effect of slumping on DOC delivery to streams is much different on the Peel Plateau than for other regions studied to date (Vonk et al., 2013a, 2013b; Abbott et al., 2014; Drake et al., 2015; Larouche et al., 2015; Mann et al., 2015; Spencer et al., 2015), it appears that the fate and overall lability of permafrost-origin carbon in this region follows similar trends to that of other Arctic regions.

These results demonstrate that changes in DOC concentrations are not reflective of the full impacts of thaw slumps on stream ecosystems and carbon cycling. This lack of correlation between changes in concentration and lability has been seen in some Alaskan regions (Balcarczyk et al., 2009) but a positive relationship has been found in others (Holmes et al., 2008; Abbott et al., 2014; Mann et al., 2014). This inconsistent relationship demonstrates the influence of a multitude of factors on BDOC, therefore suggesting that that use of basic DOC concentration measurement to infer BDOC is unreliable and should not be used when quantifying permafrost carbon cycling dynamics. ΔDOC is an important value to consider when examining the western Canadian Arctic in a global context, as the magnitude of DOC concentrations in this region are less than in other Arctic regions (Balcarczyk et al., 2009; Woods et al., 2011; Vonk et al., 2013a; Abbott et al., 2014; Drake et al., 2015; Spencer et al., 2015). Compared to absolute changes in DOC following incubations in other regions, ΔDOC was relatively low in magnitude on the Peel Plateau; one exception to this trend was HD, which displayed large ΔDOC (Fig 3.2).

BDOC values across the Peel Plateau are moderate to high when compared to Arctic regions unimpacted by significant permafrost degradation (Kawahigashi et al., 2004; Mann et al., 2012; Wickland et al., 2012). However, in comparison with other thermokarst features in Siberia (Vonk et al., 2013a, 2013b; Drake et al., 2015; Mann et al., 2015; Spencer et al., 2015) and Alaska (Abbott et al., 2014; Larouche et al., 2015), BDOC on the Peel Plateau is relatively low. Our maximum BDOC value was 33.4%, which is considerably lower than the mean BDOC values in Alaska and Siberia (Vonk et al., 2013a; Abbott et al.,

2014), where BDOC values as great as 58.2% have been reported (Drake et al., 2015; Spencer et al., 2015). One of the main hypotheses for lower BDOC in this region is the adsorption of a portion of the carbon pool to suspended mineral soils which are prevalent across the Peel Plateau (Kothawala et al., 2012). Total suspended sediments drastically increase with slump activity (Fig. 2.2; Bowden et al., 2008; Thompson et al., 2008; Kokelj et al., 2013; Malone et al., 2013), providing the opportunity for rapid adsorption to occur (Qualls & Haines, 1992; Kothawala et al., 2009, 2012).

3.5.2 Impacts of thaw slump morphology on BDOC

The influence of slump age and activity on DOC biodegradability is apparent when examining variations in BDOC across slump features (Fig. 3.3). In the larger slumps (FM2, FM3 and FM4) downstream values are marginally greater than upstream BDOC values; this is not true at SD, which is the only slump to have much greater BDOC levels downstream compared to within the slump. SD is an outlier in this study as it is the most recently established slump with a shallow headwall that is receding rapidly within the surficial permafrost layer (Table 2.1). Over the course of the summer the streamflow carved a tunnel feature through the ice rich permafrost and it was this outflow that was sampled. The greater downstream BDOC and ΔDOC suggests that the sampling regime did not capture all the slump inputs to the stream ecosystem at SD, mostly likely due to this tunnel feature.

3.5.3 BDOC response to experimental manipulations

Q_{10} is the sensitivity of DOC degradation to changes in temperatures. The calculated Q_{10} response was not statistically different ($F_{2,28}$=1.584, p=0.223) between upstream, within-slump and downstream sampling locations, in part because upstream DOC response to temperature increase showed wide variation compared to other sampling locations (Fig. 3.4b). Absolute ΔDOC differences also showed no statistical differences ($F_{2,28}$=2.119, p=0.139), though within-slump BDOC exhibited much greater variation (Fig 3.4a). Temperature increases did have a small positive effect on DOC loss at all sampling locations, as evidenced by an overall positive Q_{10} value. These results are similar to summer Q_{10} values in the Yukon River, Alaska (Wickland et al., 2012). While these increases in response to temperature seems intuitive, no or minimal temperature impacts on DOC loss have been recorded in other Arctic incubations on thermokarst features (Balcarczyk et al., 2009; Mann et al., 2015). In unimpacted Arctic streams temperature effects have been observed and are strongly influenced by seasonality (Balcarczyk et al., 2009; Wickland et al., 2012).

Nutrient release, particularly as inorganic nitrogen, from thawing permafrost has been observed in all Arctic regions (Harden et al., 2012; Harms & Jones, 2012; Reyes et al., 2015; Abbott et al., 2016).

Thermokarst features release nutrients impacting local stream systems (Bowden et al., 2008; Abbott et al., 2014, 2015) and this nutrient availability is predicted to be an important control on BDOC (Wickland et al., 2012). An increase in BDOC has been recorded in incubation experiments subject to nutrient amendments (Marschner & Kalbitz, 2003; McDowell et al., 2006), though other studies have shown that the increase in BDOC with a nutrient amendment only occurs after the removal of more aromatic compounds from the carbon pool (Mann et al., 2014). Nutrient additions to our incubations were based on measured nutrient values in the Arctic Ocean (Simpson et al. 2008), the eventual destination of Peel Plateau waters. Even though the nutrient additions in this study were relatively modest, they still led to a significant and consistent increase in BDOC (Fig. 3.4). However, the effects of nutrients are not always clear cut in the Arctic. For example, seasonality influences nutrient addition impacts on BDOC (Holmes et al., 2008), and nutrient additions have been found to have mixed effects, including no effect, on DOC degradation (Holmes et al., 2008; Balcarczyk et al., 2009; Abbott et al., 2014). These variable trends suggest that nutrient limitation is not the main influence on DOC degradation in all regions (Abbott et al., 2014). Knowing how DOC responds to temperature and nutrient increases during degradation is important as these variables are changing as a result of climate change and within thermokarst features (Williamson et al., 1999; Bowden et al., 2008; Frey & McClelland, 2009; Abbott et al., 2015). There is evidence that the increasing temperatures and nutrient fluxes predicted for Arctic regions (Harden et al., 2012; Harms & Jones, 2012; Reyes et al., 2015; Abbott et al., 2016) will increase the hydrological lability of mobilized permafrost DOC, across landscapes and especially in thermokarst impacted systems.

3.5.4 Overall drivers of BDOC on the Peel Plateau

In addition to the manipulated incubation conditions, results of the multiple linear regression showed that there are intrinsic drivers of BDOC on the Peel Plateau. $\delta^{18}O$ data from within-slump runoff exhibits older source signatures and arose as a significant driver of BDOC (Table 3.5), this trend of older sourced carbon being more susceptible to biological degradation is well established within the literature (Kawahigashi et al., 2004; Mann et al., 2012, 2014; Wickland et al., 2012; Abbott et al., 2014; Drake et al., 2015; Larouche et al., 2015; Spencer et al., 2015; Fig. 3.6). Within-slump sites also displayed much larger variations between slumps and sample periods in BDOC and $\delta^{18}O$ compared to both downstream and upstream sites (Fig. 3.5), demonstrating that even on the Peel Plateau, permafrost and BDOC patterns are highly variable. In many other studies, seasonality, assessed in this study as Julian date, influences DOC availability, flux and composition along with BDOC (Neff et al., 2006; Spencer et al., 2008; Townsend-Small et al., 2011; Wickland et al., 2012). While the sampling for this study only occurred over a two month summer thaw season, Julian date was a positive driver of BDOC (Table 3.5).

Spectral characteristics of S_R and $SUVA_{254}$ also showed strong correlations with BDOC. S_R shows a strong correlation with molecular weight (Helms et al., 2008), while $SUVA_{254}$ correlates well with DOM aromaticity (Weishaar & Aiken, 2003). In this study S_R had a strong positive relationship (R^2=0.57, p=<0.001) with BDOC and $SUVA_{254}$ had a strong negative relationship (R^2= 0.67, p=<0.001), indicating that DOC composition, characterized by spectral properties (S_R and $SUVA_{254}$), influences rates of degradation. The strong negative correlation between $SUVA_{254}$ and BDOC has also been observed in other permafrost regions, therefore in permafrost regions where sampling is difficult optical properties can act as a relatively reliable proxy for lability (McDowell et al., 2006; Fellman et al., 2008; Wickland et al., 2012; Abbott et al., 2014; Drake et al., 2015; Mann et al., 2015).

3.5.5 The eventual fate of permafrost DOC on the Peel Plateau

Numerous studies have reported that DOC mobilized from permafrost displays older signatures and has increased biolability (Kawahigashi et al., 2004; Mann et al., 2012, 2014; Wickland et al., 2012; Abbott et al., 2014; Drake et al., 2015; Larouche et al., 2015; Spencer et al., 2015; Fig. 3.6) and is preferentially degraded compared to younger carbon sources (Raymond & Bauer, 2001; Vonk et al., 2013a; Spencer et al., 2015). This is especially relevant in regards to thaw slump features, as the DOC mobilized from deep permafrost can be rapidly utilized, demonstrated by the lack of a permafrost signature in higher order streams in other regions (Vonk et al., 2013a, 2015b; Spencer et al., 2015). These findings highlight the importance of small order and thermokarst outlet studies to accurately assess BDOC dynamics in Arctic aquatic ecosystems. While DOC biodegradability is less pronounced in western Canadian Arctic thaw slumps compared to thermokarst features of other regions, BDOC levels from thaw slumps are still significantly elevated in comparison to surficial waters on the Peel Plateau and Arctic regions in general (Fig. 3.3). Therefore it is expected that the western Canadian Arctic will undergo the impacts of increased carbon cycling along with other Arctic regions, but likely at a lower magnitude.

The hydrological lability of slump mobilized permafrost DOC is dependent on its environment, which changes during transport through downstream recipient systems to the Arctic Ocean. The lability of permafrost DOC is expected to increase during terrestrial transit as streams and rivers temperatures can reach up to 19 ^{o}C (Arctic Great Rivers Observatory, 2014) and nutrients are funnelled from land to aquatic systems (Holmes et al., 2012), providing an ideal degradation environment. Studies have shown that rapid degradation (< seven days) of permafrost carbon occurs (Vonk et al., 2013b; Drake et al., 2015; Spencer et al., 2015); as the estimated transit time to the Arctic Ocean for waters draining the Peel Plateau is approximately one week, much of the potential degradation would occur within the

stream and river systems of the landscape. Once the carbon reaches the Arctic Ocean, DOC degradation is likely to be similar to BDOC values of the Env+N incubation as this incubation was designed to mimic oceanic conditions. In the regression determining the driving factors of degradation in the control incubation, nutrients were determined to be a stronger driver of BDOC compared to incubation temperature (Table 3.5), therefore it would suggest that changes to the nutrient dynamics during transit would have a larger impact on the DOC degradation rates. There are ecological and biological implications of increased carbon flux and degradation in the Arctic Ocean, especially if the carbon is readily bioavailable. Increases in carbon influx can lead to greater bacteria-organic matter coupling in the Arctic Ocean, which influences broad scale carbon cycling, microbial communities and food web dynamics (Azam et al., 1993; Kirchman et al., 2009).

There are many hypotheses for the high lability of permafrost DOC (Vonk et al., 2013a; Abbott et al., 2014). Most relevant to the western Canadian Arctic is the preferential sorption of recalcitrant carbon species to mineral soils (Kawahigashi et al., 2004, 2006; Kothawala et al., 2012) leaving the remaining DOC pool much more labile. Biolabile DOC could also be comprised of microbial biomass as microbial activity can occur below freezing but is not respired (Wilhelm et al., 2012). Low levels of pre-processing before burial could lead to compositional differences in DOC including lower molecular weights and a decrease in aromatics, which are much easier to degrade (Dutta et al., 2006; Waldrop et al., 2010; Vonk et al., 2013a; Drake et al., 2015). It is clear that further DOC composition investigations are needed to investigate the mechanisms behind the high biolability of permafrost DOC. As the Arctic continues to warm, assessing the reactivity of permafrost carbon on a regional scale is important in creating accurate regional and global carbon budgets, as thermokarst mobilized carbon degradation rates are influenced by a plethora of variables, many of which are region dependent.

3.6 Figures

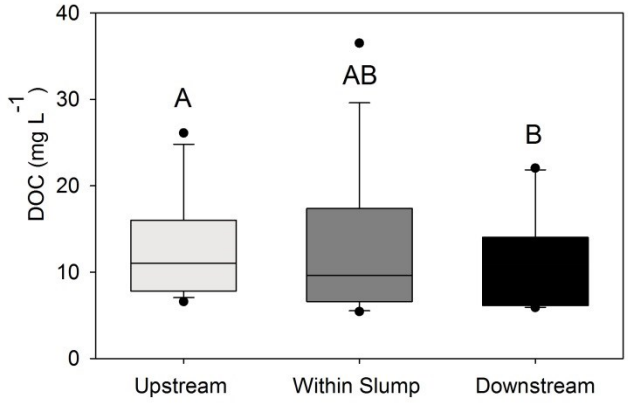

Figure 3.1 Dissolved organic carbon (DOC) concentrations across all slumps and time periods included in biodegradable DOC incubations. Separated points are outliers.

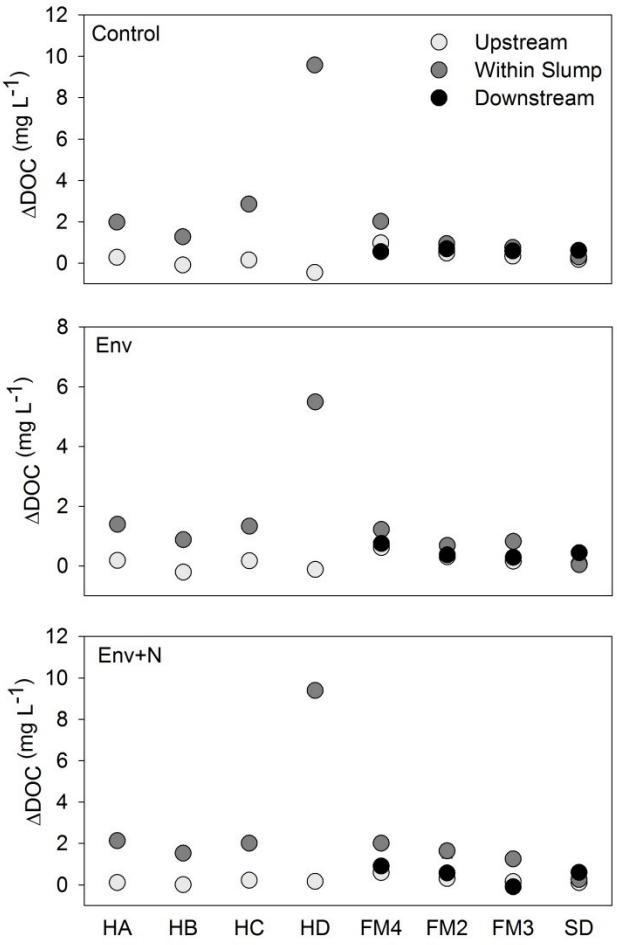

Figure 3.2 ΔDOC (absolute dissolved organic carbon loss (mg L^{-1})) across all slumps. Sites HA, HB, HC, and HD are averaged over a single time period (P2) and FM3 is the average of two time periods (P1 and P2). The remainder of the slumps are an average of all three sampling periods. Error bars are present and represent standard error (*n* explained above).

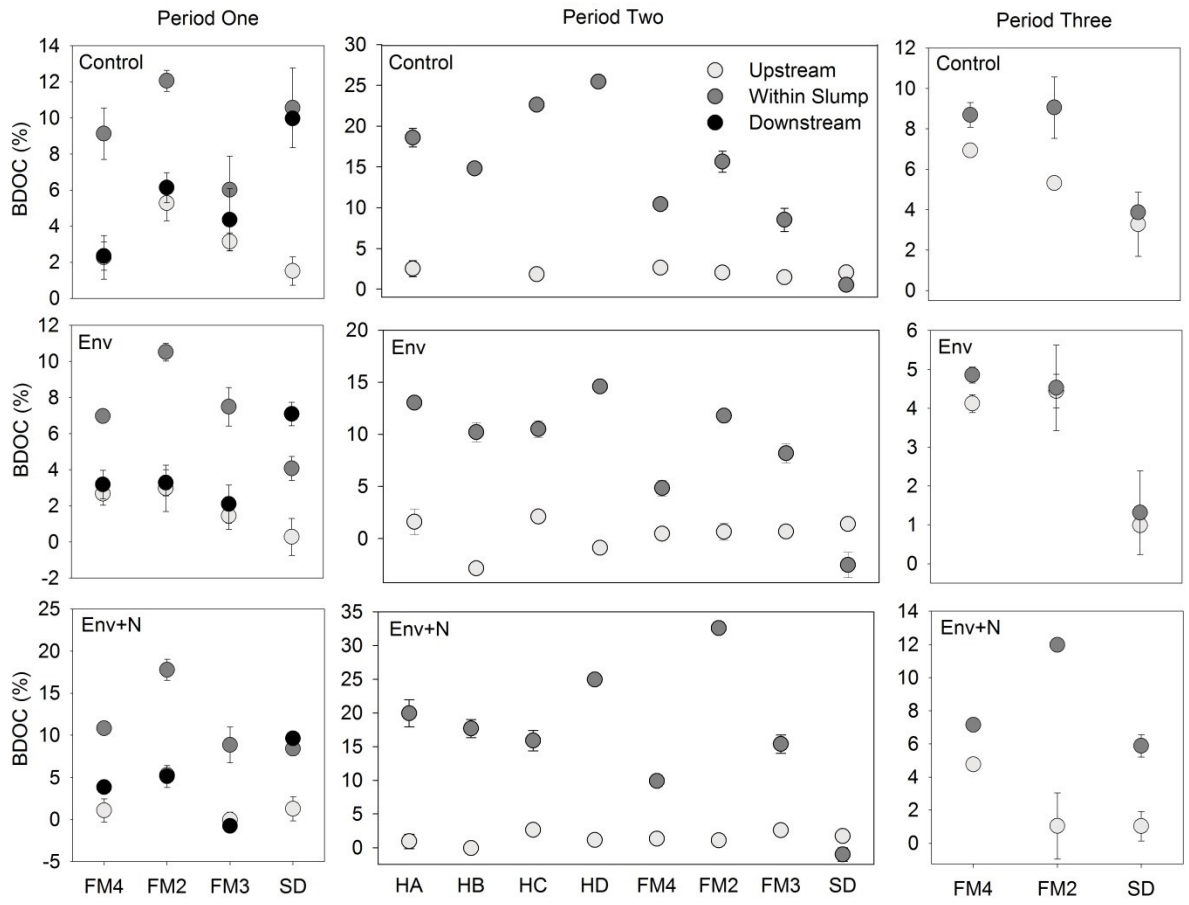

Figure 3.3 Individual slump BDOC (% loss of dissolved organic carbon) shown for individual periods and incubation types. The incubation treatments are control: 20°C for 28 days, Env: 6.4°C for 28 days and Env+N: 6.4°C for 28 days with a nutrient addition that is representative of maximum nutrient concentrations in the Beaufort Sea. Error bars represent standard error (n=3).

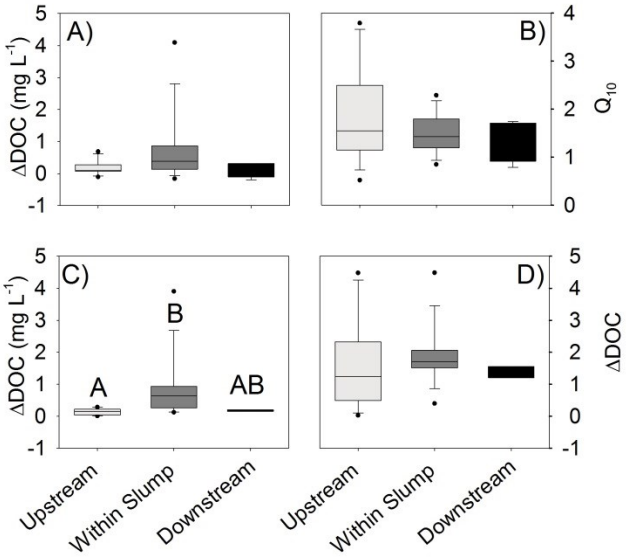

Figure 3.4 BDOC temperature and nutrient addition responses. A) Absolute differences in ΔDOC (mg L^{-1}) between the control and Env incubations. B) Q_{10} as a controlled measure of temperature sensitivity (T_1= 6.4ºC; T_2=19.5ºC). C) Absolute difference in ΔDOC (mg L^{-1}) between Env+N and Env incubations. D) Proportional ΔDOC (mg L^{-1}) differences between Env+N and Env incubations. Significant differences were followed by Tukey post hoc tests ($p < 0.001$).

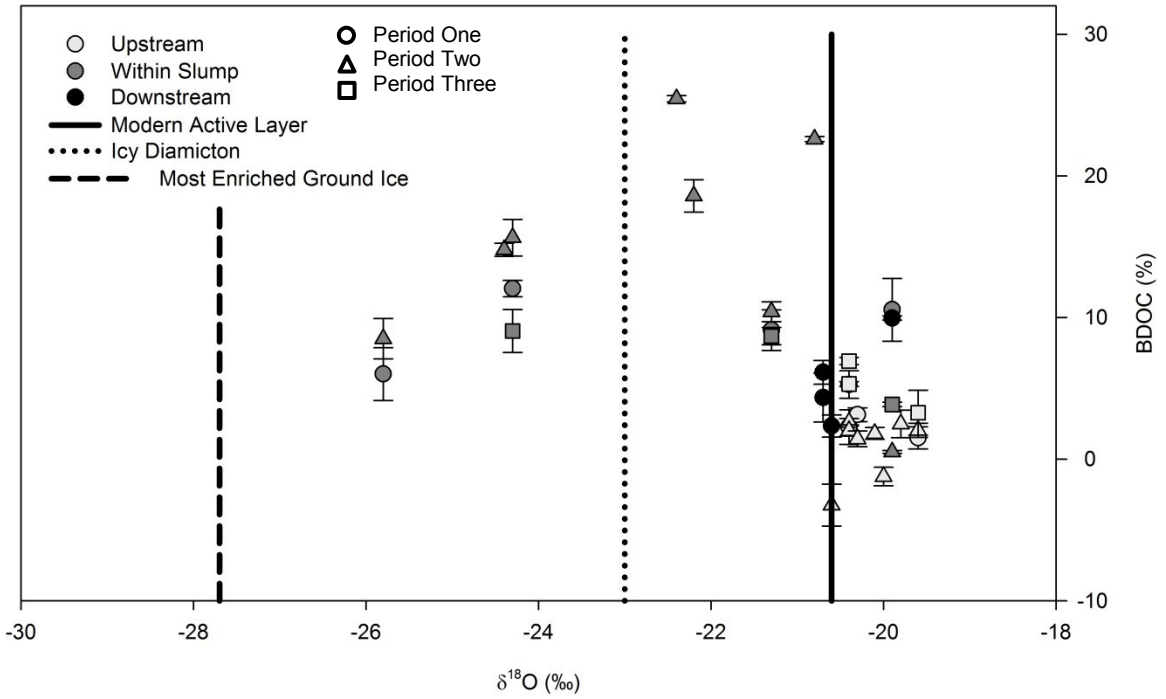

Figure 3.5 Oxygen isotope data ($\delta^{18}O‰$) is plotted against BDOC levels. References levels are taken from Lacelle et al. (2013). The modern active layer is equivalent ot the meteoric water line, icy diamicton is has been aged to be Holocene era, the most enriched ground ice value is the highest isotopic value for Pleistocene-aged ground ice presented (Lacelle et al., 2013).

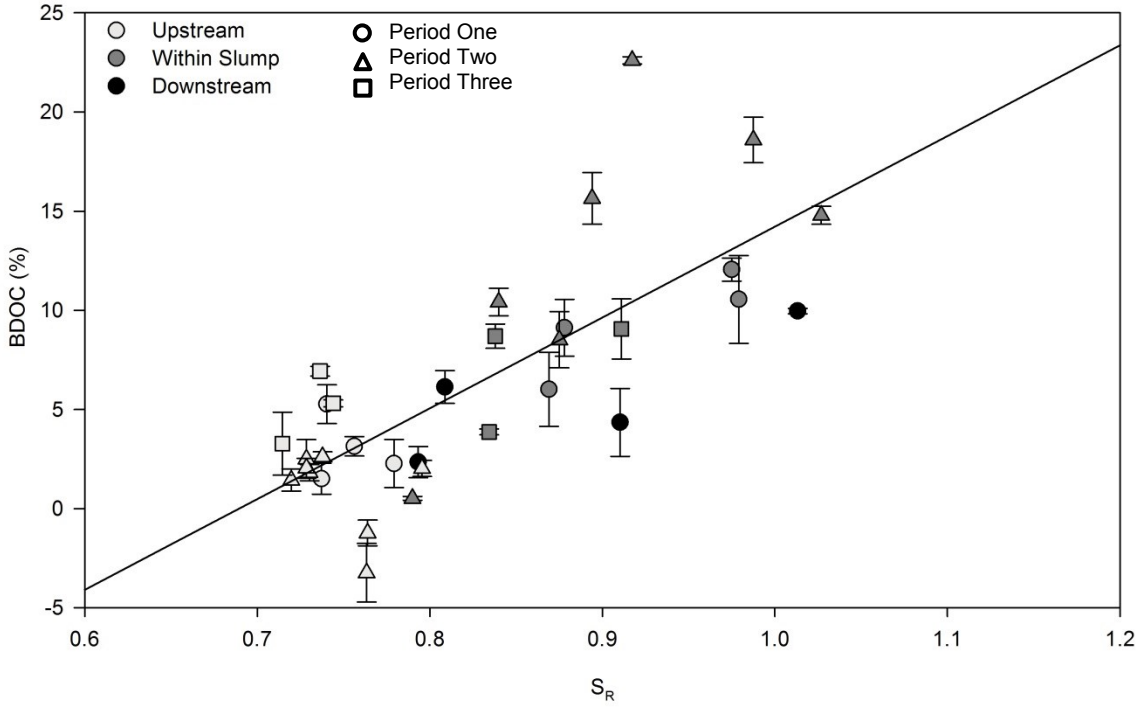

Figure 3.6 Slope ratio (S_R) plotted against biodegradable dissolved organic carbon (BDOC), with line of best fit indicated (R^2=0.57, p=<0.001). This correlation demonstrates that optical properties can be a suitable proxy for BDOC in permafrost regions. Error bars represent standard error (n=3).

3.7 Tables

Table 3.1 An overview of the various incubation treatments undertaken using slump runoff, and upstream water from the Peel Plateau, NT.

Treatment	Temperature (°C) Goal	Temperature (°C) Actual	Length of Incubation (days)	Nutrient Addition	Rationale
Control	20	19.5 ± 0.05	28	No	Standard methodology, comparison purposes
Env	7	6.4 ± 0.04	28	No	Mimics natural conditions
Env+N	7	6.4 ± 0.04	28	Yes	Mimics natural conditions at the terminus of the watershed

Table 3.2 Nutrient additions for the Env+N incubation treatment. Concentrations are maximum levels found in the Beaufort Sea (Simpson et al., 2008), the terminus for waters draining from the Peel Plateau.

Nutrient	Concentration (µmol L^{-1})
Nitrate	17.3
Phosphate	1.8
Ammonium	2.1

Table 3.3 Results from two-way ANOVAs of BDOC over three incubations, separated by sampling period. Significant interactions were found between slump and location were found for all but two of the ANOVAs and were followed by simple contrasts and simple interactions (Table 3.4).

Period One	Control			Env			Env+N		
	df	*F*	p-value	*df*	*F*	p-value	*df*	*F*	p-value
Slump	3	6.14	**0.003**	3	3.31	**0.0372**	3	19.68	**<0.001**
Location	2	26.99	**<0.001**	2	43.23	**<0.001**	2	83.09	**<0.001**
Slump:Location	6	3.41	**0.014**	6	7.79	**<0.001**	6	8.16	**<0.001**
Error	24			24			24		

Period Two	Control			Env			Env+N		
	df	*F*	p-value	*df*	*F*	p-value	*df*	*F*	p-value
Slump	7	32.90	**<0.001**	7	27.16	**<0.001**	7	58.35	**<0.001**
Location	1	1053.47	**<0.001**	1	436.45	**<0.001**	1	1155.12	**<0.001**
Slump:Location	7	63.09	**<0.001**	7	30.99	**<0.001**	7	64.23	**<0.001**
Error	31			29			31		

Period Three	Control			Env			Env+N		
	df	*F*	p-value	*df*	*F*	p-value	*df*	*F*	p-value
Slump	2	11.81	**0.0015**	2	16.77	**<0.001**	2	5.67	**0.019**
Location	1	7.00	**0.021**	1	0.50	0.498	1	58.98	**<0.001**
Slump:Location	2	1.44	0.275	2	0.12	0.887	2	10.35	**0.002**
Error	12			12			12		

Table 3.4 Simple effects and contrasts for control, Env and Env+N incubations; undertaken when higher-order interactions were significant for the two-way ANOVA (the interaction effect was not significant for the control and Env treatments during Period 3). Simple effect analyses were conducted at each slump level, and followed by simple contrasts, when three location levels were sampled.

Period One	Control				Env			Env+N		
	df	F	p value	contrasts	df	F	p value	df	F	p value	contrasts
SA	2	15.32	**<0.001**	W>D=U*	2	32.73	**<0.001**	2	21.37	**<0.001**	W>D=U*
SB	2	24.00	**<0.001**	W>D=U*	2	68.64	**<0.001**	2	44.70	**<0.001**	W>U=D*
SC	2	6.36	**0.006**	W=D=U*	2	34.18	**<0.001**	2	24.33	**<0.001**	W>U=D*
SD	2	30.09	**<0.001**	W=D>U*	2	36.48	**<0.001**	2	17.27	**<0.001**	D=W>U*
Error	24				24			24			

Period Two	Control				Env			Env+N			
	df	F	p value	contrasts	df	F	p value	df	F	p value	contrasts
HA	1	402.86	**<0.001**	W>U	1	233.20	**<0.001**	1	380.03	**<0.001**	W>U
HB	1	278.82	**<0.001**	W>U	1	214.98	**<0.001**	1	305.28	**<0.001**	W>U
HC	1	351.88	**<0.001**	W>U	1	90.45	**<0.001**	1	139.41	**<0.001**	W>U
HD	1	848.76	**<0.001**	W>U	1	405.09	**<0.001**	1	595.62	**<0.001**	W>U
SA	1	125.35	**<0.001**	W>U	1	32.37	**<0.001**	1	91.01	**<0.001**	W>U
SB	1	285.55	**<0.001**	W>U	1	194.59	**<0.001**	1	1020.81	**<0.001**	W>U
SC	1	84.03	**<0.001**	W>U	1	92.81	**<0.001**	1	218.90	**<0.001**	W>U
SD	1	4.84	**0.035**	W>U	1	14.37	**<0.001**	1	4.63	**0.039**	W>U
Error	31				29			31			

Period Three	Env+N			
	df	F	p value	contrasts
SA	1	3.06	0.106	W=U
SB	1	63.94	**<0.001**	W>U
SD	1	12.58	**<0.001**	W>U
Error	12			

***** Simple effects followed by simple contrasts

Table 3.5 Results from the multiple linear regressions determining overall drivers of variation in BDOC. The regression analysis examined the influence of slump characteristics ($\delta^{18}O$, TDN, and S_R), incubation settings (temperature and nutrient addition) and sampling regime (Julian Date) on DOC degradation (AIC= 1313.47, R^2=0.5532, $F_{6,392}$=80.9, p-value=0).

Coefficient	Estimate	t-value	p-value
$\delta^{18}O$ (‰)	-0.59	-2.89	0.004
Total Dissolved Nitrogen (N µg L^{-1})	<0.001	3.85	<0.001
Slope Ratio (S_R)	43.6	13.37	<0.001
Incubation Temperature (°C)	.25	5.20	<0.001
Nutrient Addition (presence/absence)	3.94	6.23	<0.001
Julian Date	0.04	2.54	0.012

4.0 General Conclusions

4.1 Research conclusions

The overarching result of this study is that the mobilization of DOC from retrogressive thaw slumps in the western Canadian Arctic differs from trends found in other Arctic regions. In Chapter Two we determined that slumps do impact stream systems that they feed into, and that precipitation is the largest factor in DOC mobilization from thaw slumps. In Chapter Three we showed that BDOC was greater in slump impacted streams when compared to unimpacted ones. Measured biolability was greater in carbon derived from slump runoff; if climatic trends continue as projected, increasing permafrost thaw and permafrost carbon mobilization, this degradation potential will increase with the predicted climate change (Vonk et al., 2013a). Despite this, BDOC levels in the Peel Plateau were found to be lower than in other thermokarst impacted streams from throughout the pan-Arctic (Vonk et al., 2013a, 2013b; Abbott et al., 2014; Drake et al., 2015; Larouche et al., 2015; Mann et al., 2015; Spencer et al., 2015).

Our study is the first to examine BDOC trends in the western Canadian Arctic and to inspect the direct effect that environmental variables have on DOC mobilization within this region. The overarching interest in this field of research is the examination of Arctic carbon cycles to determine if the Arctic will become a carbon source or sink with climate change (Woods et al., 2011). This work adds to a growing body of research demonstrating that the Arctic is incredibly heterogeneous, and that DOC and BDOC trends vary in magnitude and directionality across regions.

This work also focuses on the importance of identifying 'hotspots' of high carbon degradation across Arctic landscapes, as much permafrost carbon is degraded before it reaches main waterways (Mann et al., 2014, 2015). Increased levels of degradation occur in thaw slumps; so, while thaw slumps are less common than other thermokarst features across landscapes, they impact large areas and remain active for decades (Lantz et al., 2009; Kokelj & Jorgenson, 2013).

4.2 Future research directions

This research prompts several avenues of future research. First, it is important to be able to accurately compare BDOC and carbon dynamics between regions so we push for the adoption and maintenance of

a standard BDOC methodology as proposed by Vonk et al. (2015). Measurements of direct compositional differences in permafrost-derived carbon would be beneficial in explaining the enhanced lability of this carbon being observed across Arctic regions, and could potentially aid in predicting specific carbon dynamics. A modelling expansion of slump mobilized DOC response to permafrost degradation would be valuable in predicting carbon responses to future climate changes. With the decrease in DOC concentrations after slump activity, seen in the Peel Plateau, investigations into particulate organic carbon concentrations and degradation experiments are crucial, especially in the Western Canadian Arctic due to the expected adsorption to mineral soils. Another important next step for obtaining a complete depiction of carbon dynamics in Arctic ecosystems is an investigation of photo degradation influences on permafrost DOC on the Peel Plateau and elsewhere (e.g., Cory et al., 2013).

4.3 Research Improvements

For future research projects similar to this I would suggest a quantification of slump morphology, as it appears to strongly influence the carbon dynamics mobilizing from the thaw slump. A classification system of the slumps could be designed based on size, activity level and vegetation coverage. Based on this study, we would expect the most labile carbon to be present in large slumps with deep headwalls, high activity levels and low levels of vegetation. Knowledge of the depth of the active layer and permafrost layers would help explain the different patterns in DOC and isotopic signatures from each slump presented in this paper. Along these lines, carbon dating of the slump runoff would be beneficial in explicitly confirming that the permafrost carbon has the high biolability that we are presenting. Discharge calculations for each of the slumps would also be beneficial in estimating DOC loadings from the landscape to aquatic systems and would allow for an expansion of the environmental correlation regression. In the mineral soils of the Peel Plateau it would be expected that DOC concentrations would be less in all slump impacted streams when compared to pristine streams and this would be inversely correlated with total suspended sediments.

Improvements to this research design would include the continuation of the downstream sampling for all time periods as these results are what matters for the ecosystem and shows the uniqueness of mineral rich regions in regards to carbon dynamics. A more balanced sampling design would have led to much easier statistical analyses. In field sampling could have been improved through designated time at the beginning of the field season to test out sampling methodologies, as helicopter samples were lost a s a result of an in-field change in sampling protocol.

5.0 Literature cited

Abbott B.W., Jones J., Schuur E., Chapin III F.S., Bowden W., Bret-Harte M., Epstein H., Flannigan M., Harms T., Hollingworth T., Mack M., McGuire A.D., Natal S., Rocha A., Tank S., Turetsky M., Vonk J.E., Wickland K.P., Aiken G.R., Alexander H., Amon R.M.W., & Welker J. (2016) Biomass offsets little or none of permafrost carbon release from soils, streams, and wildfire: an expert assessment. *Environmental Research Letters*, **11**, 034014.

Abbott B.W., Jones J.B., Godsey S.E., Larouche J.R., & Bowden W.B. (2015) Patterns and persistence of hydrologic carbon and nutrient export from collapsing upland permafrost. *Biogeosciences*, **12**, 3725–3740.

Abbott B.W., Larouche J.R., Jones J.B., Bowden W.B., & Balser A.W. (2014) Elevated dissolved organic carbon biodegradability from thawing and collapsing permafrost. *Journal of Geophysical Research*, **119**, 2049–2063.

Arctic Great Rivers Observatory (2014) PARTNERS Project Arctic River Biogeochemistry Data Set. (NSF–1107774).

Aufdenkampe A.K., Mayorga E., Raymond P.A., Melack J.M., Doney S.C., Alin S.R., Aalto R.E., & Yoo K. (2011) Riverine coupling of biogeochemical cycles between land, oceans, and atmosphere. *Frontiers in Ecology and the Environment*, **9**, 53–60.

Azam F., Smith D.C., Steward G.F., & Hagstrom A. (1993) Bacteria-organic matter coupling and its significance for oceanic carbon cycling. *Microbial Ecology*, **28**, 167–179.

Balcarczyk K.L., Jones J.B., Jaffé R., & Maie N. (2009) Stream dissolved organic matter bioavailability and composition in watersheds underlain with discontinuous permafrost. *Biogeochemistry*, **94**, 255–270.

Battin T.J., Kaplan L.A., Findlay S., Hopkinson C.S., Marti E., Packman A.I., Newbold J.D., & Sabater F. (2008) Biophysical controls on organic carbon fluxes in fluvial networks. *Nature Geoscience*, **1**, 95–100.

Bowden W.B., Gooseff M.N., Balser A., Green A., Peterson B.J., & Bradford J. (2008) Sediment and nutrient delivery from thermokarst features in the foothills of the North Slope, Alaska: Potential impacts on headwater stream ecosystems. *Journal of Geophysical Research: Biogeosciences*, **113**,

1–12.

Brooker A., Fraser R.H., Olthof I., Kokelj S. V., & Lacelle D. (2014) Mapping the activity and evolution of retrogressive thaw slumps by tasselled cap trend analysis of a Landsat satellite image stack. *Permafrost and Periglacial Processes*, **25**, 243–256.

Burn C.R. & Kokelj S. V (2009) The environment and permafrost of the Mackenzie Delta area. *Permafrost and Periglacial Processes*, **20**, 83–105.

Burn C.R. & Lewkowicz A.G. (1990) Canadian Landform Examples - 17: Retrogressive thaw slumps. *The Canadian Geographer*, **34**, 273–76.

Burnham K.P. & Anderson D.R. (2002) *Model Selection and Multi- Model Inference: A Practical Information-Theoretic Approach.* Springer, New York.

Carmack E.C., Macdonald R.W., & Jasper S. (2004) Phytoplankton productivity on the Canadian Shelf of the Beaufort Sea. *Marine Ecology Progress Series*, **277**, 37–50.

Carpenter S.R., Cole J.J., Kitchell J.F., & Pace M.L. (1998) Impact of dissolved organic carbon, phosphorus, and grazing on phytoplankton biomass and production in experimental lakes. *Limnology and Oceanography*, **43**, 73–80.

Catto N.R. (1996) Richardson Mountains, Yukon-Northwest territories: The northern portal of the postulated "Ice-Free Corridor." *Quaternary International*, **32**, 3–19.

Cogley J.G. & McCann S.B. (1976) An exceptional storm and its effects in the Canadian High Arctic. *Arctic and Alpine Research*, **8**, 105–110.

Cole J.J., Prairie Y.T., Caraco N.F., McDowell W.H., Tranvik L.J., Striegl R.G., Duarte C.M., Kortelainen P., Downing J.A., Middelburg J.J., & Melack J. (2007) Plumbing the global carbon cycle: Integrating inland waters into the terrestrial carbon budget. *Ecosystems*, **10**, 171–184.

Cory R.M., Crump B.C., Dobkowski J.A., & Kling G.W. (2013) Surface exposure to sunlight stimulates CO2 release release from permafrost soil carbon in the Arctic. *Proceedings of the National Academy of Sciences of the United States of America*, **110**, 3429–3434.

Curtin J. (2015) lmSupport: Support for Linear Models. R package version 2.9.2. http://CRAN.R-project.org/package=lmSupport.

Dittmar T. & Kattner G. (2003) The biogeochemistry of the river and shelf ecosystem of the Arctic Ocean: a review. *Marine Chemistry*, **83**, 103–120.

Drake T.W., Wickland K.P., Spencer R.G.M., McKnight D.M., & Striegl R.G. (2015) Ancient low–molecular-weight organic acids in permafrost fuel rapid carbon dioxide production upon thaw. *Proceedings of the National Academy of Sciences*, **112**, 13946–13951.

Duk-Rodkin A. & Hughes O.L. (1992) Surficial geology, Fort McPherson-Bell River. Yukon-Northwest Territories. Geological Survey of Canada, Map 1745A, scale 1:250 000.

Durbin J. & Watson G.S. (1950) Testing for serial correlation in least squares regression I. *Biometrika*, **37**, 409–428.

Dutta K., Schuur E.A.G., Neff J.C., & Zimov S.A. (2006) Potential carbon release from permafrost soils of Northeastern Siberia. *Global Change Biology*, **12**, 2336–2351.

Environment Canada (2015) Canadian Climate Normals 1981-2010 Station Data, Fort McPherson. http://climate.weather.gc.ca.

van Everdingen (Ed.) R. (1998) *Multi-language glossary of permafrost and related ground-ice terms.* International Permafrost Association,The University of Calgary Printing Services, Calgary, Canada, 311 p.

Fellman J.B., D'Amore D. V., Hood E., & Boone R.D. (2008) Fluorescence characteristics and biodegradability of dissolved organic matter in forest and wetland soils from coastal temperate watersheds in southeast Alaska. *Biogeochemistry*, **88**, 169–184.

Fox J. & Weisberg S. (2011) An {R} Companion to Applied Regression, Second Edition. Thousand Oaks CA: Sage. URL: http://socserv.socsci.mcmaster.ca/jfox/Books/Companion.

Frey K.E. & McClelland J.W. (2009) Impacts of permafrost degradation on arctic river biogeochemistry. *Hydrological Processes*, **23**, 169–182.

Frey K.E. & Smith L.C. (2005) Amplified carbon release from vast West Siberian peatlands by 2100. *Geophysical Research Letters*, **32**, 1–4.

Fritz M., Opel T., Tanski G., Herzschuh U., Meyer H., Eulenburg A., & Lantuit H. (2015) Dissolved organic carbon (DOC) in Arctic ground ice. *The Cryosphere*, **9**, 737–752.

Green S.A. & Blough N. V. (1994) Optical absorption and fluorescence properties of chromophoric dissolved organic matter in natural waters. *Limnology and Oceanography*, **39**, 1903–1916.

Grom J.D. & Pollard W.H. (2008) A study of High Arctic retrogressive thaw slump dynamics, Eureka Sound Lowlands, Ellesmere Island In: Kane, D.L., Hinkel, K.M. (Eds.), Proceedings of the Ninth International Conference on Permafrost. Institute of Northern Engineering, University of Alaska. *Ninth International Conference on Permafrost*, pp. 545–550.

Gross J. & Ligges U. (2015) nortest: Tests for Normality. R package version 1.0-4. http://CRAN.R-project.org/package=nortest.

Grosse G., Romanovsky V., Jorgenson T., Walter Anthony K., Brown J., & Overduin P.P. (2011) Vulnerability and feedbacks of permafrost to climate change. *EOS, Transactions, American Geophysical Union.*, **92**, 73–80.

Hair J.F.J., Anderson R.E., Tatham R.L., & Black W.C. (1995) *Multivariate Data Analysis.* Macmillan, New York.

Hanson P.C., Bade D.L., Carpenter S.R., & Kratz T.K. (2003) Lake metabolism: Relationships with dissolved organic carbon and phosphorus. *Limnology and Oceanography*, **48**, 1112–1119.

Harden J.W., Koven C.D., Ping C.L., Hugelius G., David McGuire A., Camill P., Jorgenson T., Kuhry P., Michaelson G.J., O'Donnell J.A., Schuur E.A.G., Tarnocai C., Johnson K., & Grosse G. (2012) Field information links permafrost carbon to physical vulnerabilities of thawing. *Geophysical Research Letters*, **39**, 1–6.

Harms T.K. & Jones J.B. (2012) Thaw depth determines reaction and transport of inorganic nitrogen in valley bottom permafrost soils: Nitrogen cycling in permafrost soils. *Global Change Biology*, **18**, 2958–68.

Helms J.R., Stubbins A., Ritchie J.D., Minor E.C., Kieber D.J., & Mopper K. (2008) Absorption spectral slopes and slope ratios as indicators of molecular weight, source, and photobleaching of chromophoric dissolved organic matter. *Limnology and Oceanography*, **53**, 955–969.

Hessen D.O. (1992) Dissolved organic carbon in a humic lake: effects on bacterial production and respiration. *Hydrobiologia*, **229**, 115–123.

Hinzman L.D., Deal C.J., Mcguire a. D., Mernild S.H., Polyakov I. V., & Walsh J.E. (2013) Trajectory of the Arctic as an integrated system. *Ecological Applications*, **23**, 1837–1868.

Holmes R.M., McClelland J.W., Peterson B.J., Tank S.E., Bulygina E., Eglinton T.I., Gordeev V. V., Gurtovaya T.Y., Raymond P.A., Repeta D.J., Staples R., Striegl R.G., Zhulidov A. V., & Zimov S.A. (2012) Seasonal and annual fluxes of nutrients and organic matter from large rivers to the Arctic Ocean and surrounding seas. *Estuaries and Coasts*, **35**, 369–382.

Holmes R.M., McClelland J.W., Raymond P.A., Frazer B.B., Peterson B.J., & Stieglitz M. (2008) Lability of DOC transported by Alaskan rivers to the Arctic Ocean. *Geophysical Research Letters*, **35**, 1–5.

Hugelius G., Strauss J., Zubrzycki S., Harden J.W., Schuur E.A.G., Ping C.L., Schirrmeister L., Grosse G., Michaelson G.J., Koven C.D., O'Donnell J.A., Elberling B., Mishra U., Camill P., Yu Z., Palmtag J., & Kuhry P. (2014) Estimated stocks of circumpolar permafrost carbon with quantified uncertainty ranges and identified data gaps. *Biogeosciences*, **11**, 6573–6593.

Hugelius G., Tarnocai C., Broll G., Canadell J.G., Kuhry P., & Swanson D.K. (2013) The northern circumpolar soil carbon database: Spatially distributed datasets of soil coverage and soil carbon storage in the northern permafrost regions. *Earth System Science Data*, **5**, 3–13.

Hughes O.L., Hodgson D.A., & Pilon J. (1972) Surficial geology, Fort Good Hope, Arctic Red River, Fort McPherson, District of Mackenzie, maps and legend; Geological Survey of Canada, Open File 97, scale 1:125,000.

IPCC (2014) Climate Change 2014: Synthesis Report. Contribution of Working Groups I, II and III to the Fifth Assessment Report of the Intergovernmental Panel on Climate Change [Core Writing Team, R.K. Pachauri and L.A. Meyer (eds.)]. IPCC, Geneva, Switzerland, 151 pp.

Jin H., Yu Q., Lu L., Guo D., He R., Yu S., Sun G., & Li Y. (2007) Degradation of Permafrost in the Xing ' anling Mountains , Northeastern China. *Permafrost and Periglacial Processes*, **18**, 245–258.

Jorgenson M.T., Romanovsky V., Harden J., Shur Y., O'Donnell J., Scuur E.A.G., Kanevskiy M., & Marchenko S. (2010) Resilience and vulnerability of permafrost to climate change. *Canadian Journal of Forest Research*, **40**, 1219–1236.

Jorgenson M.T., Shur Y.L., & Pullman E.R. (2006) Abrupt increase in permafrost degradation in Arctic Alaska. *Geophysical Research Letters*, **33**, 2–5.

Kalbitz K., Schmerwitz J., Schwesig D., & Matzner E. (2003) Biodegradation of soil-derived dissolved organic matter as related to its properties. *Geoderma*, **113**, 273–291.

Kawahigashi M., Kaiser K., Kalbitz K., Rodionov A., & Guggenberger G. (2004) Dissolved organic matter in small streams along a gradient from discontinuous to continuous permafrost. *Global Change Biology*, **10**, 1576–1586.

Kawahigashi M., Kaiser K., Rodionov A., & Guggenberger G. (2006) Sorption of dissolved organic matter by mineral soils of the Siberian forest tundra. *Global Change Biology*, **12**, 1868–1877.

Keller K., Blum J.D., & Kling G.W. (2010) Stream geochemistry as an indicator of increasing permafrost thaw depth in an arctic watershed. *Chemical Geology*, **273**, 76–81.

Keppel G. & Wickens T.D. (2004) *Design and analysis: a researcher's handbook.* Pearson Prentice Hall, Upper Saddle River, New Jersey, U.S.A.

Khvorostyanov D. V., Ciais P., Krinner G., Zimov S.A., Corradi C., & Guggenberger G. (2008a) Vulnerability of permafrost carbon to global warming. Part II: Sensitivity of permafrost carbon stock to global warming. *Tellus, Series B: Chemical and Physical Meteorology*, **60 B**, 265–275.

Khvorostyanov D. V., Krinner G., Ciais P., Heimann M., & Zimov S.A. (2008b) Vulnerability of permafrost carbon to global warming. Part I: Model description and role of heat generated by organic matter decomposition. *Tellus, Series B: Chemical and Physical Meteorology*, **60 B**, 250–264.

Kirchman D.L., Moran X.A.G., & Ducklow H. (2009) Microbial growth in the polar oceans-role of temperature and potential impact of climate change. *Nature Reviews Microbiology*, **7**, 451–459.

Kokelj S. V. & Burn C.R. (2003) Ground ice and soluble cations in near-surface permafrost, Inuvik, Northwest Territories, Canada. *Permafrost and Periglacial Processes*, **14**, 275–289.

Kokelj S. V., Jenkins R.E., Milburn D., Burn C.R., & Snow N. (2005) The influence of thermokarst disturbance on the water quality of small upland lakes, Mackenzie Delta region, Northwest Territories, Canada. *Permafrost and Periglacial Processes*, **16**, 343–353.

Kokelj S. V. & Jorgenson M.T. (2013) Advances in thermokarst research. *Permafrost and Periglacial Processes*, **24**, 108–119.

Kokelj S. V., Lacelle D., Lantz T.C., Tunnicliffe J., Malone L., Clark I.D., & Chin K.S. (2013) Thawing of

massive ground ice in mega slumps drives increases in stream sediment and solute flux across a range of watershed scales. *Journal of Geophysical Research: Earth Surface*, **118**, 681–692.

Kokelj S. V., Lantz T.C., Kanigan J.C., Smith S.L., & Coutts R. (2009) Origin and polycyclic behaviour of tundra thaw slumps, Mackenzie Delta region, Northwest Territories, Canada. *Permafrost and Periglacial Processes*, **20**, 173–184.

Kokelj S. V., Smith C.A.., & Burn C.R. (2002) Physical and chemical characteristics of the active layer and permafrost, Herschel Island, western Arctic Coast, Canada. *Permafrost and Periglacial Processes*, **13**, 171–185.

Kokelj S.V., Tunnicliffe J., Lacelle D., Lantz T.C., Chin K.S., & Fraser R. (2015) Increased precipitation drives mega slump development and destabilization of ice-rich permafrost terrain, northwestern Canada. *Global and Planetary Change*, **129**, 56–68.

Kothawala D.N., Moore T.R., & Hendershot W.H. (2008) Adsorption of dissolved organic carbon to mineral soils: A comparison of four isotherm approaches. *Geoderma*, **148**, 43–50.

Kothawala D.N., Moore T.R., & Hendershot W.H. (2009) Soil properties controlling the adsorption of dissolved organic carbon to mineral soils. *Soil Science Society of America Journal*, **73**, 1831.

Kothawala D.N., Roehm C., Blodau C., & Moore T.R. (2012) Selective adsorption of dissolved organic matter to mineral soils. *Geoderma*, **189-190**, 334–342.

Lacelle D., Bjornson J., & Lauriol B. (2010) Climatic and geomorphic factors affecting contemporary (1950-2004) activity of retrogressive thaw slumps on the Aklavik plateau, Richardson mountains, NWT, Canada. *Permafrost and Periglacial Processes*, **21**, 1–15.

Lacelle D., Brooker A., Fraser R.H., & Kokelj S. V. (2015) Distribution and growth of thaw slumps in the Richardson Mountains–Peel Plateau region, northwestern Canada. *Geomorphology*, **235**, 40–51.

Lacelle D., Lauriol B., Zazula G., Ghaleb B., Utting N., & Clark I.D. (2013) Timing of advance and basal condition of the Laurentide Ice Sheet during the last glacial maximum in the Richardson Mountains, NWT. *Quaternary Research (United States)*, **80**, 274–283.

Lafrenière M.J. & Lamoureux S.F. (2013) Thermal perturbation and rainfall runoff have greater impact on seasonal solute loads than physical disturbance of the active layer. *Permafrost and Periglacial*

Processes, **24**, 241–251.

Lamoureux S.F. & Lafreniére M.J. (2009) Fluvial impact of extensive active layer detachments, Cape Bounty, Melville Island, Canada. *Arctic, Antarctic, and Alpine Research*, **41**, 59–68.

Lantuit H. & Pollard W.H. (2005) Temporal stereophotogrammetric analysis of retrogressive thaw slumps on Herschel Island, Yukon Territory. *Natural Hazards and Earth System Science*, **5**, 413–423.

Lantuit H. & Pollard W.H. (2008) Fifty years of coastal erosion and retrogressive thaw slump activity on Herschel Island, southern Beaufort Sea, Yukon Territory, Canada. *Geomorphology*, **95**, 84–102.

Lantz T.C., Kokelj S. V., Gergel S.E., & Henry G.H.R. (2009) Relative impacts of disturbance and temperature: persistent changes in microenvironment and vegetation in retrogressive thaw slumps. *Global Change Biology*, **15**, 1664–1675.

Larouche J.R., Abbott B.W., Bowden W.B., & Jones J.B. (2015) The role of watershed characteristics, permafrost thaw, and wildfire on dissolved organic carbon biodegradability and water chemistry in Arctic headwater streams. *Biogeosciences*, **12**, 4221–4233.

Laudon H., Buttle J., Carey S.K., McDonnell J., McGuire K., Seibert J., Shanley J., Soulsby C., & Tetzlaff D. (2012) Cross-regional prediction of long-term trajectory of stream water DOC response to climate change. *Geophysical Research Letters*, **39**, 4–9.

Lee C.L. & Kuo L.J. (1999) Quantification of the dissolved organic matter effect on the sorption of hydrophobic organic pollutant: Application of an overall mechanistic sorption model. *Chemosphere*, **38**, 807–821.

Lewkowicz A.G. (1985) Use of an ablatometer to measure short-term ablation of exposed ground ice. *Canadian Journal of Earth Sciences*, **22**, 1767–1773.

Lewkowicz A.G. (1986) Rate of short-term ablation of exposed ground ice, Banks Island, Northwest Territories, Canada. *Journal Of Glaciology*, **32**, 511–519.

Lewkowicz A.G. (1987) Headwall retreat of ground-ice slumps, Banks Island, Northwest Territories. *Canadian Journal of Earth Sciences*, **24**, 1077–1085.

Lewkowicz A.G. (1990) Morphology, frequency and magnitude of active-layer detachment slides, Fosheim Peninsula, Ellesmere Island, N.W.T. *Final Proceedings, Fifth Canadian Permafrost*

Conference, 111–118.

Lewkowicz A.G. & Harris C. (2005) Morphology and geotechnique of active-layer detachment failures in discontinuous and continuous permafrost, northern Canada. *Geomorphology*, **69**, 275–297.

MacDougall A.H., Avis C. a., & Weaver A.J. (2012) Significant contribution to climate warming from the permafrost carbon feedback. *Nature Geoscience*, **5**, 719–721.

Mackay J.R. (1971) The origin of massive icy beds in permafrost, Western Arctic Coast, Canada. *Nature*, **8**, 397–422.

MacLean R., Oswood M.W., Irons J.G., & McDowell W.H. (1999) The effect of permafrost on stream biogeochemistry: A case study of two streams in the Alaskan (U.S.A.) taiga. *Biogeochemistry*, **47**, 239–267.

Malone L., Lacelle D., Kokelj S., & Clark I.D. (2013) Impacts of hillslope thaw slumps on the geochemistry of permafrost catchments (Stony Creek watershed, NWT, Canada). *Chemical Geology*, **356**, 38–49.

Mann P.J., Davydova A., Zimov N., Spencer R.G.M., Davydov S., Bulygina E., Zimov S., & Holmes R.M. (2012) Controls on the composition and lability of dissolved organic matter in Siberia's Kolyma River basin. *Journal of Geophysical Research: Biogeosciences*, **117**, 1–15.

Mann P.J., Eglinton T.I., McIntyre C.P., Zimov N., Davydova A., Vonk J.E., Holmes R.M., & Spencer R.G.M. (2015) Utilization of ancient permafrost carbon in headwaters of Arctic fluvial networks. *Nature Communications*, **6**, DOI: 10.1038/ncomms8856.

Mann P.J., Sobczak W. V., LaRue M.M., Bulygina E., Davydova A., Vonk J.E., Schade J., Davydov S., Zimov N., Holmes R.M., & Spencer R.G.M. (2014) Evidence for key enzymatic controls on metabolism of Arctic river organic matter. *Global Change Biology*, **20**, 1089–1100.

Marschner B. & Kalbitz K. (2003) Controls of bioavailability and biodegradability of dissolved organic matter in soils. *Geoderma*, **113**, 211–235.

McDowell W.H., Zsolnay A., Aitkenhead-Peterson J.A., Gregorich E.G., Jones D.L., Jödemann D., Kalbitz K., Marschner B., & Schwesig D. (2006) A comparison of methods to determine the biodegradable dissolved organic carbon from different terrestrial sources. *Soil Biology and Biochemistry*, **38**, 1933–1942.

McGuire A.D., Anderson L.G., Christensen T.R., Dallimore S., Guo L., Hayes D.J., Heimann M., Lorenson T.D., MacDonald R.W., & Roulet N. (2009) Sensitivity of the carbon cycle in the Arctic to climate change. *Ecological Monographs*, **79**, 523–555.

McGuire A.D., Hayes D.J., Kicklighter D.W., Manizza M., Zhuang Q., Chen M., Follows M.J., Gurney K.R., McClelland J.W., Melillo J.M., Peterson B.J., & Prinn R.G. (2010) An analysis of the carbon balance of the Arctic Basin from 1997 to 2006. *Tellus, Series B: Chemical and Physical Meteorology*, **62**, 455–474.

Murton J. & French H. (1994) Cryostructures in permafrost, Tuktoyaktuk coastlands, western arctic Canada. *Canadian Journal of Earth Sciences*, **31**, 737–747.

Neff J.C., Finlay J.C., Zimov S.A., Davydov S.P., Carrasco J.J., Schuur E.A.G., & Davydova A.I. (2006) Seasonal changes in the age and structure of dissolved organic carbon in Siberian rivers and streams. *Geophysical Research Letters*, **33**, 1–5.

Norris D.K. (1984) Geology of the northern Yukon and northwestern District of Mackenzie. Geological Survey of Canada,Map 1581A, scale 1:500 000.

O'Donnell J.A., Aiken G.R., Kane E.S., & Jones J.B. (2010) Source water controls on the character and origin of dissolved organic matter in streams of the Yukon River basin, Alaska. *Journal of Geophysical Research: Biogeosciences*, **115**, 1–12.

O'Donnell J.A., Aiken G.R., Walvoord M.A., & Butler K.D. (2012) Dissolved organic matter composition of winter flow in the Yukon River basin: Implications of permafrost thaw and increased groundwater discharge. *Global Biogeochemical Cycles*, **26**, 1–18.

Oliva M. & Ruiz-Fernández J. (2015) Coupling patterns between para-glacial and permafrost degradation responses in Antarctica. *Earth Surface Processes and Landforms*, n/a–n/a.

Pinheiro J., Bates D., DebRoy S., Sarkar D., & R Core Team (2015) nlme: Linear and Nonlinear Mixed Effects Models. R package version 3.1-120, http://CRAN.R-project.org/package=nlme>.

Poulin B.A., Ryan J.N., & Aiken G.R. (2014) Effects of iron on optical properties of dissolved organic matter. *Environmental science & technology*, **48**, 10098–10106.

Prokushkin A.S., Kajimoto T., Prokushkin S.G., McDowell W.H., Abaimov A.P., & Matsuura Y. (2005)

Climatic factors influencing fluxes of dissolved organic carbon from the forest floor in a continuous-permafrost Siberian watershed. *Canadian Journal of Forest Research*, **35**, 2130–2140.

Pumpanen J., A L., Heli M., Kolari P., Ilvesniemi H., Mammarella I., Hari O., Nikinmaa E., Heinonsalo J., Back J., Ojala A., Berninger F., & Vesala T. (2014) Precipitation and net ecosystem exchange are the most important drivers of DOC flux in upland boreal catchments. *Journal of Geophysical Research: Biogeosciences*, **119**, 1861–1878.

Qualls R. & Haines B.L. (1992) Measuring adsorption isotherms using continuous, unsaturated flow through intact soil cores. *Soil Science Society of America Journal*, **56**, 456–460.

R Core Team (2015) *R: A Language and Environment for Statistical Computing.* R Foundation for Statistical Computing, Vienna, Austria. http://www.r-project.org/.

Raymond P.A. & Bauer J.E. (2001) Riverine export of aged terrestrial organic matter to the North Atlantic Ocean. *Letters to Nature*, **409**, 497–500.

Reyes F.R., Lougheed V.L., Rancisco F., & Reyes R. (2015) Rapid Nutrient Release from Permafrost Thaw in Arctic Aquatic Ecosystems. *Arctic, Antarctic, and Alpine Research*, **47**, 35–48.

Romanovsky V.E., Smith S.L., & Christiansen H.H. (2010) Permafrost thermal state in the polar northern hemisphere during the International Polar Year 2007-2009: A synthesis. *Permafrost and Periglacial Processes*, **21**, 106–116.

Rudy A., Lamoureux S.F., & Lantz T.C. (2015) Watershed delineation in areas of permafrost disturbance on eastern Banks Island , NWT : a geomatics approach for predicting water quality impacts.

Salonen K. & Hammar T. (1986) On the importance of dissolved organic matter in the nutrition of zooplankton in some lake waters. *Oecologia*, **68**, 246–253.

Schaefer K., Zhang T., Bruhwiler L., & Barrett A.P. (2011) Amount and timing of permafrost carbon release in response to climate warming. *Tellus, Series B: Chemical and Physical Meteorology*, **63**, 165–180.

Schneider Von Deimling T., Meinshausen M., Levermann A., Huber V., Frieler K., Lawrence D.M., & Brovkin V. (2012) Estimating the near-surface permafrost-carbon feedback on global warming. *Biogeosciences*, **9**, 649–665.

Schuur E., Bockheim J., Canadell J.G., B E.E.C., Goryachkin S. V, Hagemann S., Kuhry P., Lafleur P.M., Lee H., Nelson M.F.E., Rinke A., Romanovsky V.E., Shiklomanov N., Tarnocai C., Venevsky S., Vogel J.G., & Sergei A. (2008) Vulnerability of permafrost carbon to climate change : Implications for the global carbon cycle. *BioScience*, **58**, 701–714.

Schuur E.A.G., Abbott B.W., Bowden W.B., Brovkin V., Camill P., Canadell J.G., Chanton J.P., Chapin F.S., Christensen T.R., Ciais P., Crosby B.T., Czimczik C.I., Grosse G., Harden J., Hayes D.J., Hugelius G., Jastrow J.D., Jones J.B., Kleinen T., Koven C.D., Krinner G., Kuhry P., Lawrence D.M., McGuire A.D., Natali S.M., O'Donnell J.A., Ping C.L., Riley W.J., Rinke A., Romanovsky V.E., Sannel A.B.K., Schädel C., Schaefer K., Sky J., Subin Z.M., Tarnocai C., Turetsky M.R., Waldrop M.P., Walter Anthony K.M., Wickland K.P., Wilson C.J., & Zimov S.A. (2013) Expert assessment of vulnerability of permafrost carbon to climate change. *Climatic Change*, **119**, 359–374.

Schuur E.A.G., McGuire A.D., Grosse G., Harden J.W., Hayes D.J., Hugelius G., Koven C.D., & Kuhry P. (2015) Climate change and the permafrost carbon feedback. *Nature*, **520**, 171–179.

Simpson K.G., Tremblay J.É., Gratton Y., & Price N.M. (2008) An annual study of inorganic and organic nitrogen and phosphorus and silicic acid in the southeastern Beaufort Sea. *Journal of Geophysical Research: Oceans*, **113**, 1–16.

Slater A.G. & Lawrence D.M. (2013) Diagnosing present and future permafrost from climate models. *Journal of Climate*, **26**, 5608–5623.

Smith S.L., Burgess M.M., Riseborough D., & Nixon F.M. (2005) Recent trends from Canadian permafrost thermal monitoring network sites. *Permafrost and Periglacial Processes*, **16**, 19–30.

Spencer R.G.M., Aiken G.R., Butler K.D., Dornblaser M.M., Striegl R.G., & Hernes P.J. (2009) Utilizing chromophoric dissolved organic matter measurements to derive export and reactivity of dissolved organic carbon exported to the Arctic Ocean: A case study of the Yukon River, Alaska. *Geophysical Research Letters*, **36**, 1–6.

Spencer R.G.M., Aiken G.R., Wickland K.P., Striegl R.G., & Hernes P.J. (2008) Seasonal and spatial variability in dissolved organic matter quantity and composition from the Yukon River basin, Alaska. *Global Biogeochemical Cycles*, **22**, 1–13.

Spencer R.G.M., Mann P.J., Dittmar T., Eglinton T.I., Mcintyre C., Holmes R.M., Zimov N., & Stubbins A.

(2015) Detecting the signature of permafrost thaw in Arctic rivers. *Geophysical Research Letters*, **42**, doi:10.1002/2015GL063498.

Striegl R.G., Aiken G.R., Dornblaser M.M., Raymond P.A., & Wickland K.P. (2005) A decrease in discharge-normalized DOC export by the Yukon River during summer through autumn. *Geophysical Research Letters*, **32**, 1–4.

Tank S.E., Frey K.E., Striegl R.G., Raymond P.A., Holmes R.M., McClelland J.W., & Peterson B.J. (2012) Landscape-level controls on dissolved carbon flux from diverse catchments of the circumboreal. *Global Biogeochemical Cycles*, **26**, 1–16.

Tarnocai C., Canadell J.G., Schuur E.A.G., Kuhry P., Mazhitova G., & Zimov S. (2009) Soil organic carbon pools in the northern circumpolar permafrost region. *Global Biogeochemical Cycles*, **23**, 1–11.

Thompson M.S., Prowse T.D., Kokelj S. V, & Wrona F.J. (2008) The impact of sediments derived from thawing permafrost on tundra lake water chemistry: An experimental approach. *Proceedings of the Ninth International Conference on Permafrost*, **29**, 1763–1768.

Townsend-Small A., McClelland J.W., Holmes R.M., & Peterson B.J. (2011) Seasonal and hydrologic drivers of dissolved organic matter and nutrients in the upper Kuparuk River, Alaskan Arctic. *Biogeochemistry*, **103**, 109–124.

Tranvik L.J. (1988) Availability of dissolved organic carbon for planktonic bacteria in oligotrophic lakes of differing humic content. *Microbial Ecology*, **16**, 311–322.

Vonk J.E. & Gustafsson Ö. (2013) Permafrost-carbon complexities. *Nature Geoscience*, **6**, 675–676.

Vonk J.E., Mann P.J., Davydov S., Davydova A., Spencer R.G.M., Schade J., Sobczak W. V., Zimov N., Zimov S., Bulygina E., Eglinton T.I., & Holmes R.M. (2013a) High biolability of ancient permafrost carbon upon thaw. *Geophysical Research Letters*, **40**, 2689–2693.

Vonk J.E., Mann P.J., Dowdy K.L., Davydova A., Davydov S.P., Zimov N., Spencer R.G.M., Bulygina E.B., Eglinton T.I., & Holmes R.M. (2013b) Dissolved organic carbon loss from Yedoma permafrost amplified by ice wedge thaw. *Environmental Research Letters*, **8**, 035023.

Vonk J.E., Tank S.E., Bowden W.B., Laurion I., Vincent W.F., Alekseychik P., Amyot M., Billet M.F., Canário J., Cory R.M., Deshpande B.N., Helbig M., Jammet M., Karlsson J., Larouche J., Macmillan G., Rautio

M., Walter Anthony K.M., & Wickland K.P. (2015a) Reviews and syntheses: Effects of permafrost thaw on Arctic aquatic ecosystems. *Biogeosciences*, **12**, 7129–7167.

Vonk J.E., Tank S.E., Mann P.J., Spencer R.G.M., Treat C.C., Striegl R.G., Abbott B.W., & Wickland K.P. (2015b) Biodegradability of dissolved organic carbon in permafrost soils and waterways: a meta-analysis. *Biogeosciences*, **12**, 6915–6930.

Waldrop M.P., Wickland K.P., White R., Berhe A.A., Harden J.W., & Romanovsky V.E. (2010) Molecular investigations into a globally important carbon pool: Permafrost-protected carbon in Alaskan soils. *Global Change Biology*, **16**, 2543–2554.

Walsh J.E., Overland J.E., Groisman P.Y., & Rudolf B. (2011) *Snow, Water, Ice and Permafrost in the Arctic (SWIPA): Climate Change and the Cryosphere.* Arctic Monitoring and Assessment Programme (AMAP), Oslo, Norway.

Walvoord M.A. & Striegl R.G. (2007) Increased groundwater to stream discharge from permafrost thawing in the Yukon River basin : Potential impacts on lateral export of carbon and nitrogen. *Geophysical Research Letters*, **34**, doi:10.1029/2007GL030216. 1.

Wang B., Paudel B., & Li H. (2009) Retrogression characteristics of landslides in fine-grained permafrost soils, Mackenzie Valley, Canada. *Landslides*, **6**, 121–127.

Ward R.C. & Robinson M. (2000) *Principles of Hydrology.* McGraw-Hill International (UK) Limited,

Weishaar J. & Aiken G. (2003) Evaluation of specific ultra-violet absorbance as an indicator of the chemical content of dissolved organic carbon. *Environmental Chemistry*, **37**, 4702–4708.

Wickland K.P., Aiken G.R., Butler K., Dornblaser M.M., Spencer R.G.M., & Striegl R.G. (2012) Biodegradability of dissolved organic carbon in the Yukon River and its tributaries: Seasonality and importance of inorganic nitrogen. *Global Biogeochemical Cycles*, **26**, 1–14.

Wilhelm R.C., Radtke K.J., Mykytczuk N.C.S., Greer C.W., & Whyte L.G. (2012) Life at the Wedge: the Activity and Diversity of Arctic Ice Wedge Microbial Communities. *Astrobiology*, **12**, 347–360.

Williamson C.E., Morris D.P., Pace M.L., & Olson O.G. (1999) Dissolved organic carbon and nutrients as regulators of lake ecosystems: Resurrection of a more integrated paradigm. *Limnology and Oceanography*, **44**, 795–803.

Woods G.C., Simpson M.J., Pautler B.G., Lamoureux S.F., Lafrenière M.J., & Simpson A.J. (2011) Evidence for the enhanced lability of dissolved organic matter following permafrost slope disturbance in the Canadian High Arctic. *Geochimica et Cosmochimica Acta*, **75**, 7226–7241.

Zar J.H. (2010) *Bioststistical Analysis.* Pearson Prentice Hall, Upper Saddle River, New Jersey, U.S.A.

Zeileis A. & Grothendieck G. (2005) zoo: S3 Infrastructure for Regular and Irregular Time Series. *Journal of Statistical Software*, **14**, 1–27.

Zeileis A. & Hothorn T. (2002) Diagnostic checking in regression relationships. *R News*, **2**, 7–10.

Zuur A.F., Ieno E.N., Walker N., Saveliev A.A., & Smith G.M. (2009) *Mixed effects models and extensions in ecology with R.* Springer, New York.